

Review

C. elegans Apical Extracellular Matrices Shape Epithelia

Jennifer D. Cohen  and Meera V. Sundaram * 

Department of Genetics, University of Pennsylvania Perelman School of Medicine 415 Curie Blvd,
Philadelphia, PA 19104-6145, USA; jencohen@pennmedicine.upenn.edu

* Correspondence: sundaram@pennmedicine.upenn.edu

Received: 4 July 2020; Accepted: 27 August 2020; Published: 6 October 2020



Abstract: Apical extracellular matrices (aECMs) coat exposed surfaces of epithelia to shape developing tissues and protect them from environmental insults. Despite their widespread importance for human health, aECMs are poorly understood compared to basal and stromal ECMs. The nematode *Caenorhabditis elegans* contains a variety of distinct aECMs, some of which share many of the same types of components (lipids, lipoproteins, collagens, zona pellucida domain proteins, chondroitin glycosaminoglycans and proteoglycans) with mammalian aECMs. These aECMs include the eggshell, a glycocalyx-like pre-cuticle, both collagenous and chitin-based cuticles, and other understudied aECMs of internal epithelia. *C. elegans* allows rapid genetic manipulations and live imaging of fluorescently-tagged aECM components, and is therefore providing new insights into aECM structure, trafficking, assembly, and functions in tissue shaping.

Keywords: *C. elegans*; apical extracellular matrix; cuticle; eggshell; glycocalyx

1. Introduction

1.1. Apical Extracellular Matrix

Animals contact their environment via epithelial tissues, which create an impermeable barrier that separates the outside environment from the inside. The exposed outer surfaces of epithelia are coated with an apical extracellular matrix (aECM) that serves as a first line of defense against desiccation, pathogens, xenobiotics, and other environmental insults. Considerable evidence indicates that aECMs are also crucial for shaping epithelia, including biological tubes [1]. For example, aECMs such as the glycocalyx and surfactant maintain the narrow tubes of the mammalian blood vasculature and the lung [2,3].

Epithelia are polarized cells, with a basal surface facing the inside of the body and an apical surface facing the external environment or inside of biological tubes. Extracellular matrices that line the apical surfaces are distinct from those that line basal surfaces [4]. Basal surfaces are lined by basement membranes, extracellular matrices that form stiff, collagen-, laminin- and glycoprotein-rich sheets [4,5]. Apical surfaces are lined by diverse types of aECMs, which are laminar structures formed of lipid, sugar, and protein components [6–8]. By their repulsion of water, lipids protect against desiccation and hydrophilic small molecules [9,10]. Glycosaminoglycans, proteoglycans, and glycoproteins such as mucins may bind water molecules to swell and expand apical compartments, and may also prevent pathogens from accessing the apical membrane [8]. Fibril-forming proteins, such as collagens and Zona Pellucida (ZP) proteins, or carbohydrates such as chitin, can provide stiffness to shape apical surfaces and can assemble solid extracellular structures to form invertebrate cuticles [11–14].

Despite the importance of aECMs, the assembly mechanisms and compositions of aECM layers remain unclear. Functions of aECM are often inferred based on broad enzymatic removal or genetic

depletion of entire glycosylation or lipid biosynthesis pathways. Thus, functions of individual matrix components are rarely described. Mechanisms by which aECMs affect cell shape also remain relatively obscure. For example, unlike basement membranes, which are known to impact the cytoskeleton via binding to integrins [5], it is not clear how most aECMs are anchored to the plasma membrane or whether they influence the cytoskeleton.

This lack of knowledge regarding aECM biology is due in part to challenges in visualizing aECMs, which are often translucent and invisible by standard light microscopy and are easily damaged by fixation protocols [15]. *Caenorhabditis elegans* is a genetically tractable model organism that allows rapid assessment of individual gene requirements and live imaging of fluorescently-tagged aECM components, and is therefore providing new insights into aECM structure, assembly and functions in tissue shaping.

1.2. *Caenorhabditis elegans* as a Model Organism for Studying Apical ECMs

The nematode *C. elegans* has several features that make it an attractive model system for studying animal aECMs. *C. elegans* contains aECMs with many of the same components (lipids, lipoproteins, collagens, ZP proteins, mucins, glycosaminoglycans, and proteoglycans) as mammalian aECMs, but it also has chitin-rich aECMs that may be more similar to those found in insects. *C. elegans* is optically transparent, enabling live imaging of these aECMs. Tubes of different sizes that nevertheless contain similar aECMs allow dissection of aECM function. Finally, powerful forward and reverse genetic approaches allow identification of key aECM components.

C. elegans generates many different types of aECMs in its various tissues and across its lifespan. Despite a maximum size of about 1 mm in length and only 959 somatic cells in the adult, *C. elegans* has a wide variety of epithelial cell types, each with their own aECMs. The *C. elegans* life cycle contains six stages: embryo stage (E), four larval stages (L1–L4), and the adult (A) stage. The L2 and L3 stages are different under non-crowded, ample-food conditions, which are optimal for reproductive growth, and under non-ideal conditions such as crowding, absent food and high temperatures, when the animal forms stress-resistant dauer larvae (Figure 1) [16]. A flexible, collagenous cuticle lines most adult and larval external epithelia [17]. Between larval stages and between the L4 and adult are the molts, during which the animal synthesizes a new cuticle and sheds its old cuticle [18]. Embryos and molting larvae synthesize a transient glycoprotein-rich “pre-cuticle” between the old and new cuticles [19–22]. In addition to the cuticle and pre-cuticle, *C. elegans* has a number of other aECM types. For example, a chitinous eggshell surrounds the developing embryo [23–25], and the *C. elegans* pharynx contains a rigid chitinous cuticle with “teeth” that pulverize bacteria for digestion [25–27]. Internal epithelia such as the gut and uterus also have poorly described but intriguing non-cuticular aECMs. Below, we summarize the structures and functions of these various different aECMs.

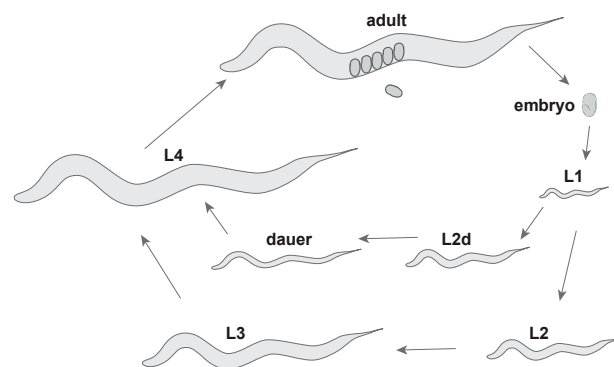


Figure 1. *C. elegans* life cycle. Adults lay embryos that hatch into L1 larvae. Larvae molt into subsequent stages. Under stress (low food, high temperatures, and crowding), larvae can molt into an alternative L3 stage called dauer, which can resume reproductive development upon return to non-stressful conditions. After Wormatlas [28].

2. The Eggshell

C. elegans embryogenesis occurs within an eggshell that both protects and shapes the developing organism. Many aspects of eggshell structure and assembly have been reviewed recently [24]. The eggshell is produced primarily by the zygote, starting immediately after fertilization of the oocyte in the spermatheca, with some contribution from the uterus [29]. The final eggshell contains five morphologically and biochemically distinct layers composed of proteins, chitin, chondroitin proteoglycans (CPGs), and lipids, plus a peri-embryonic layer that apposes the embryo [23,25,30,31] (Figure 2). Besides the peri-embryonic layer, whose relationship with the later-forming embryonic sheath is unclear, these eggshell layers are separate from the pre-cuticle matrix layers that form later around the embryo (see below).

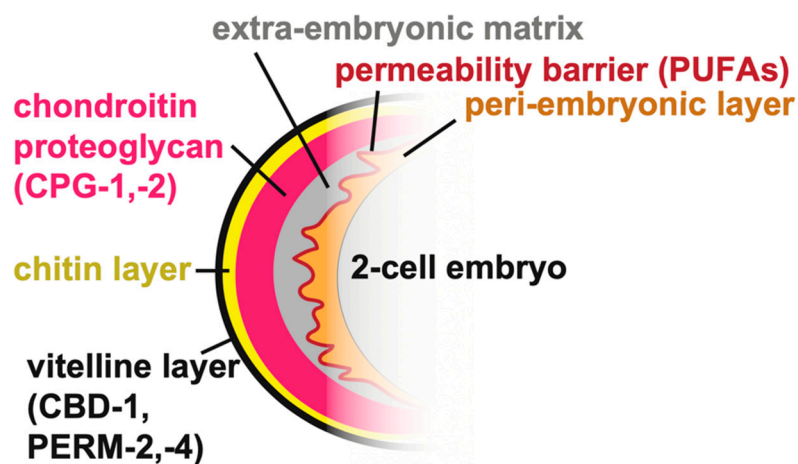


Figure 2. *C. elegans* eggshell. The outermost vitelline layer (black) contains the CBD-1/PERM-2/PERM-4 complex [31]. Next, the chitin-rich layer (yellow) is followed by the chondroitin proteoglycan layer (pink), which contains the chondroitin-proteoglycan proteins CPG-1 and CPG-2 [23]. The extra-embryonic matrix (gray) and the peri-embryonic matrix (orange), which line the embryo, are separated by the permeability barrier (red) [24,31].

2.1. Building the Eggshell

The eggshell is constructed by sequential waves of matrix secretion and deposition, with the outermost layers added first, followed by more internal layers [31]. Prior to ovulation, the vitelline layer is secreted. Upon fertilization, the vitelline layer is remodeled and a chitin-rich layer is produced beneath it [25,32]. After fertilization, meiotic progression triggers further temporally distinct steps of eggshell secretion, including delivery of cortical granules to form the chondroitin proteoglycan (CPG) layer at anaphase I and delivery of lipids to form the permeability barrier layer at anaphase II [30,31]. Finally, uterine-derived proteins can attach to the outer eggshell surface, though it is not clear if any actually incorporate into its matrix [29].

The permeability barrier layer of the eggshell is built from fatty acids imported into the developing oocyte from the mother's somatic tissues [24,31,33,34]. Loss of this permeability layer allows entry of water and small molecules through the eggshell and perturbs development of the peri-embryonic layer and the embryo [32,34]. Supplementing the animals' diet with specific poly-unsaturated fatty acids (PUFAs) rescues embryo viability and defects in the permeability barrier and peri-embryonic layer in mutants with defects in fatty acid transport [35], indicating that PUFAs may be the main components of this layer.

A few protein components of different eggshell layers have been identified. The secreted chitin binding domain protein CBD-1 and the secreted mucins PERM-2 and PERM-4 form a complex within the outermost vitelline layer [30]. CPG-1 and CPG-2 are nematode-specific chondroitin proteoglycans within the CPG layer [31]. The transmembrane extracellular leucine-rich-repeat only (eLRRon) protein

EGG-6 is a potential peri-embryonic layer component or interactor based on its mutant phenotype and its presence within the embryonic pre-cuticle [21], but its specific localization with respect to the eggshell has not yet been determined. The shared requirement for EGG-6 for both eggshell and pre-cuticle organization raises the possibility that epidermal pre-cuticle could arise in part from an earlier eggshell layer. Although ZP proteins are major components of the mammalian eggcoat [36], none have been described in the *C. elegans* eggshell.

Defects in one eggshell layer can lead to defects in assembly of subsequent layers, but not always in a predictable manner. For example, loss of the vitelline layer component CBD-1 also disrupts formation of the internal layers [30,31]. Similarly, loss of chitin leads to defects in the permeability layer [32] and loss of enzymes that produce fatty acids required for the permeability layer causes defects in the peri-embryonic layer [31–34]. On the other hand, loss of PERM-2 or PERM-4 mildly disrupts the vitelline layer and the permeability layer without greatly disturbing the overall integrity of the intervening chitin or chondroitin layers [30]. The data support a hierarchical assembly model whereby early deposited outer layers help constrain subsequently secreted factors to form inner layers, but also suggest possible communication between distantly placed layers. It is not yet clear if inner layers also could aid in remodeling or maintenance of previously secreted outer layers.

2.2. The Eggshell Shapes Early Development

The eggshell influences early stages of *C. elegans* embryogenesis. Before egg laying, the early-deposited chitin and vitelline layers stiffen the eggshell [37] and protect the new zygote from fragmenting as it transitions from the spermatheca to the uterus [32]. Mutation of key eggshell components or chemical removal of eggshell outer layers during the meiotic divisions leads to a number of severe defects in polar body extrusion, centrosome movement to the cortex, proper cell division axes, and embryo elongation [32,38–42]. Often, actin is also mislocalized, and this may drive the observed phenotypes [32,39,40], although the relationship between actin and the eggshell is not known. Chemical removal of the vitelline and chitin eggshell layers after the meiotic divisions can produce abnormal cell division polarities, likely due in part to disrupted cell–cell interactions [43–45]. In contrast, enzymatic removal of only the chitinous layer results in mild defects in embryonic elongation [46]. The eggshell likely offers a combination of mechanical structure and signaling to shape the embryo over time.

3. Pre-Cuticular aECMs

Pre-cuticular aECMs form just prior to the 1.5-fold stage of embryogenesis (Figure 3A–C), disappear prior to hatching and are replaced by cuticle, and then reappear before each larval molt [20]. A transient pre-cuticle can be detected in every tissue that later secretes collagen-based cuticle, including the epidermis and various interfacial tubes that connect the epidermis and the external environment to internal tissues.

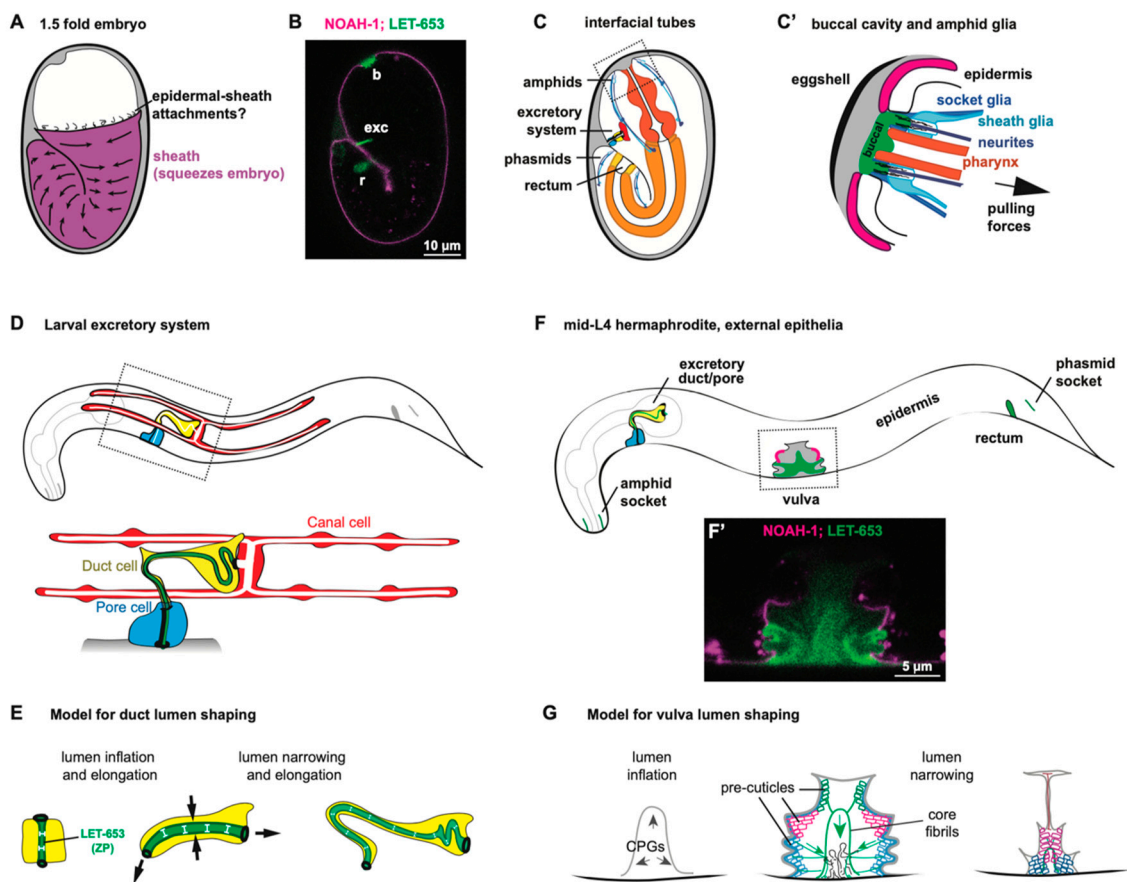


Figure 3. *C. elegans* pre-cuticles shape developing epithelia. (A) Diagram of a 1.5 fold *C. elegans* embryo encased in the embryonic sheath. The sheath distributes actinomyosin-based forces that squeeze the embryo into a worm-shape [47]. (B) Confocal image of fluorescently-tagged ZP proteins LET-653 and NOAH-1 in a 1.5 fold embryo. LET-653 (green) primarily lines interfacial tubes, including the excretory duct and pore lumen, the rectum (r), and the buccal cavity (b) [48]. NOAH-1 (magenta) is present in the embryonic sheath [47]. (C) Cross section of a 1.5-fold embryo, showing interfacial tubes. (C') The pharynx, glia, and neurites are pulled posteriorly while being anchored anteriorly by the pre-cuticle aECM [49–51]. Magenta represents NOAH-1-containing pre-cuticle, and green represents LET-653-containing pre-cuticle, as shown in in panel B. (D) The larval excretory system. The duct and pore tubes are lined by pre-cuticle and cuticle (green), while the canal tube contains a non-cuticular aECM. Black denotes junctions. (E) Model for duct lumen shaping by LET-653 and the pre-cuticle (adapted from [20]). LET-653 (green) promotes duct lumen inflation and resists morphogenetic stretching and squeezing forces (arrows) to maintain proper lumen diameter. (F) Diagram of a mid-L4 larva, showing tissues lined by pre-cuticle and cuticle. (F') Confocal image of fluorescently-tagged ZP proteins LET-653 and NOAH-1 in the L4 vulva. (G) Model for vulva lumen shaping by the pre-cuticle (adapted from [48]). After initial lumen inflation by CPGs, distinct pre-cuticles form along the apical surfaces of different vulva cell types. Connections between these pre-cuticles and a central core structure contribute to lumen narrowing.

Pre-cuticle typically contains glycoproteins of the ZP, eLRRon, and lipocalin families [20,21,47,50,52,53]. Some of these proteins reappear at each molt, and are present in many tissues, while others may be present in only a subset of tissues or stages. For example, the ZP protein NOAH-1 is strongly present in the epidermal sheath pre-cuticle but not visible in interfacial tubes of the embryo, whereas a different ZP protein, LET-653, has the converse pattern [47,52] (Figure 3B). Thus, there is no single type of pre-cuticle, but rather a set of related pre-cuticles, each specialized for a particular epithelial tissue.

Pre-cuticle aECMs are present during the major periods of epithelial morphogenesis, and play important roles in tissue shaping and in patterning the cuticles that eventually replace them. Loss of pre-cuticle components results in severe defects in body shaping, tube shaping, and cuticle structure.

3.1. The Epidermal Sheath Elongates the Embryo

The embryonic epidermal sheath overlays the epidermis and promotes embryo elongation (Figure 3A). Although the sheath was first visualized by scanning electron microscopy several decades ago [22], the first embryonic sheath components were identified more recently. These include the ZP proteins NOAH-1, NOAH-2, and FBN-1, the eLRRon proteins SYM-1, EGG-6, and LET-4, and the lipocalin LPR-3 [21,47,50,52,53]. Additional factors are seen specifically over seam cells that produce alae ridges (see below) or in interfacial tubes (LET-653, DEX-1) [20,52].

The *C. elegans* embryo elongates into a worm shape via a combination of actinomyosin-based contraction and pre-cuticle stabilization [54]. During the earliest phases of embryo elongation, actin-myosin filaments in the seam epidermis constrict circumferentially, and actin and the sheath aECM appear to reorganize together to support the new body shape [22,47,54]. Once body muscle contractions begin at the two-fold stage, these exert additional tension on the newly developed hemidesmosomes that cross the epidermis to link the sheath with underlying muscle. This tension triggers an actin severing mechanism that further shortens circumferential actin filaments throughout the epidermis [54]. In the absence of key sheath components NOAH-1 or NOAH-2, the embryo begins to elongate but then retracts and sometimes ruptures. In the absence of multiple sheath components, the remaining aECM detaches from the epidermis and muscle and even less initial elongation occurs [22,47]. Therefore, the sheath aECM is not only needed to stabilize shape changes induced by cytoskeletal forces, but also to allow those changes in the first place. Whether the aECM also generates some of the constriction force remains to be investigated.

Despite the apparent connection between the sheath aECM and hemidesmosomes, it remains unclear how they are connected across the plasma membrane. MUP-4 and MUA-3, which connect the cuticle to hemidesmosomes, are possible candidates [47,55–57]; however, their single mutant phenotypes arise later than those of sheath mutants. NOAH-1, NOAH-2 and FBN-1 do have transmembrane domains, but most ZP proteins are cleaved away from their transmembrane domains as a pre-requisite for subsequent polymerization [58]. SYM-1 and LPR-3 do not have transmembrane domains [53,59], and transgenic experiments suggested that the LET-4 transmembrane domain is not essential for its tissue-shaping functions [21]. Therefore, the relevant transmembrane linkers remain to be identified.

3.2. A Luminal Precuticle Shapes the Narrow Excretory Duct and Pore Lumens

The excretory system is an osmoregulatory organ that contains three tandem, single-celled tubes: the canal, duct, and pore cells (Figure 3D) [60,61]. The canal extends four lumenized arms along the animal's body cavity, from which it presumably exchanges osmolytes. The canal attaches to the duct cell and the duct attaches to the pore, which releases excretory contents into the outside environment.

During embryogenesis, as the tubes of the excretory system elongate, the duct and pore are lined by a set of pre-cuticular aECM components, including the lipocalin LPR-3 [53], the ZP protein LET-653 [20,48], the nidogen-domain protein DEX-1 [52], and the eLRRon proteins LET-4 and EGG-6 [21]. In addition, the lipocalin LPR-1 appears to affect the function of this aECM, but does not stably incorporate into it [62,63]. Loss of any one of these components causes lumen collapse and dilation in the duct and pore tubes, leading to fluid retention and rod-like lethality at the first larval stage; many pre-cuticle components were initially identified based on this phenotype [20,21,52,53,62,63].

How pre-cuticle shapes the duct and pore tubes remains unclear. Ectopic expression of one pre-cuticle component, LET-653, was sufficient to expand the gut lumen [20], suggesting an intrinsic, lumen-expanding activity (Figure 3E). Nevertheless, in *let-653* mutants, duct and pore luminal defects typically appear after the time that LET-653 protein would normally have been cleared,

suggesting improper assembly of later pre-cuticle or cuticle components that more directly impact lumen structure [20]. Although LET-653 re-appears within the duct during each molt cycle, its lumen shaping activity is only required in the embryo, suggesting that the pre-cuticle counters forces specifically present during morphogenesis (Figure 3E) [20]. It is possible that pre-cuticle components distribute actin-myosin-dependent contractile forces similar to the role proposed above for the epidermal sheath [54], and/or that they create a luminal scaffold around which the narrow duct lumen can elongate.

3.3. Pre-Cuticular and Sensory aECMs Anchor the Pharynx and Sensory Organs to the Epidermis

The pre-cuticle and other sensory matrix factors have a critical role in shaping the embryo's developing nervous system and buccal (mouth) cavity. The buccal cavity, at the anterior end of the pharynx, is surrounded by bundles of sensory neurites and glia forming a rosette (Figure 3C,C') [64–66]. During embryonic elongation, several aECM factors help these organs remain anchored to the anterior epidermis while the pharynx elongates and the neuronal and glial cell bodies actively migrate towards the posterior [49,50] (Figure 3C').

Three matrix proteins have been reported to shape the buccal cavity. FBN-1 is a large fibrillin-like ZP protein present within the epidermal sheath and also secreted into the buccal cavity [50,52]. DYF-7 is a neuronally-expressed ZP protein, and DEX-1 is an epithelial and glial-expressed Nidogen-and EGF-domain protein [49,52]. Loss of any of these factors can cause the buccal cavity to over-elongate and the pharynx to ingress within the worm's body during embryonic elongation [50,52,67]. FRET sensors demonstrated that the elongating pharynx exerts an inward pulling force on the anterior epidermis and buccal cavity [50]. The various ECM factors appear to resist pulling forces from morphogenesis to maintain the shape and integrity of the entire nose region (Figure 3C').

Similarly, DYF-7 and DEX-1 anchor neurites and glia to the epidermis [49,51]. Sensory neurons in the nose tip (amphid) and tail (phasmid) extend neurites into the environment through two sets of wrapping glia, the sheath and the socket, both of which have epithelial tube-like characteristics [51]. The socket glia are situated at the external body surface and are coated in a pre-cuticle or cuticle (Figure 3C'). In contrast, the neighboring sheath glia are lined by a non-cuticular aECM [51,66]. Transmission electron microscopy of embryos reveals a fibrillar matrix within the tube-like lumens of the sheath and socket glia [51]. The ZP protein DYF-7 is present in this matrix as observed by fluorescence microscopy, and in *dyf-7* mutants, much of the fibrillar structure of this matrix is absent. DYF-7 is therefore a presumed fibrillar component of this sensory-specific matrix. DYF-7 is localized to the dendrite tip by *par-6* [64] and the ciliary transition zone genes *ccep-1* and *nphp-4* [68], suggesting that multiple intercellular systems converge to attach this sensory aECM to glial cells, neurons, and to the epidermal aECM. However, the precise connections between the various cells and matrices remain to be elucidated.

The diameter of sheath and socket glia lumens also are determined in part by DYF-7 [51] and by the coordinated action of the Patched-related genes *daf-6* and *che-14*, which were proposed to regulate secretion or endocytosis of aECM factors [69–73]. *daf-6* mutants have closed sockets and expanded sheath lumens [71], while *che-14* mutants accumulate vesicles in the amphid lumen [69]. In addition, *daf-6* mutants also have *dyf-7*-like dendrite anchoring defects [74]. DAF-6 is localized to the glial apical membrane by the apically secreted PLAC-homology domain protein DYF-4, whose loss phenocopies *daf-6* mutations [74].

3.4. The Vulva Lumen Is Shaped by a Multi-Layered Pre-Cuticular aECM

The vulva is a relatively large tube that connects the uterus to the outside environment to allow for egg laying [75]. It is comprised of twenty-two cells of seven different types derived from either Ras-dependent (primary) or Notch-dependent (secondary) vulva precursor cells [76] (Figure 3F). During L4 stage, the vulva first expands dramatically from a simple invagination to a large lumen via the action of chondroitin glycosaminoglycans and actin-myosin constriction [77–82]. Next, the vulva

tube is shaped into a narrow, slit-like channel via further cell shape changes, rearrangements, and the action of its pre-cuticular aECM (Figure 3G) [48,83]. This multicellular tube is large enough to allow for the visualization, and thus the dissection, of its pre-cuticular aECM's spatial, temporal, and functional organization [48].

Chondroitin glycosaminoglycans (GAGs) are crucial for initial vulva lumen expansion (Figure 3G). Electron microscopy reveals that the inflated vulva lumen is entirely filled with a granular matrix that likely corresponds to these GAGs and CPGs [48]. Loss of chondroitin GAGs or GAG sulfation causes dramatically narrowed or “squashed” vulvas (*Sqv* phenotype) [79–81,84,85]. The current model holds that chondroitin absorbs water molecules to expand the vulva lumen like a sponge. However, in addition, chondroitin appears to work with pre-cuticle components to constrain and shape the lumen more locally [48].

GAGs are typically attached to protein carriers to form CPGs, but the relevant carriers for vulva expansion are not yet known. There may be multiple redundant carriers since none were identified in the original genetic screens for *sqv* mutants [84]. Mass spectrometry studies have identified twenty-four *C. elegans* proteins that have chondroitin GAG attachments [23,86], and at least one pre-cuticle component, *FBN-1*, is among these, but so far none of the corresponding mutants have been described to have vulva expansion defects [23,48]. Instead, *fbn-1* mutants have defects in later stages of vulva eversion [48]. Future studies of double mutants may be needed to determine which CPGs work together to inflate the vulva lumen.

Most of the pre-cuticle proteins identified to date are found in the developing vulva, and these proteins each have distinct localization patterns that mark different aECM layers lining specific vulva cell types [20,48,53]. For example, the ZP protein *LET-653* and the lipocalin *LPR-3* label slightly offset membrane-proximal pre-cuticle layers [53], whereas *LET-653* also labels a stalk-like core structure in the central part of the lumen (Figure 3F') [20,48]. Furthermore, different pre-cuticle factors label the surfaces of primary-or secondary-derived cell types at different stages (Figure 3F,F'). Vulva aECM contents change dramatically over short timeframes during tube morphogenesis, before eventually being replaced by cuticle. These reproducible spatial and temporal patterns suggest highly regulated mechanisms for pre-cuticle assembly and disassembly, and the vulva is an ideal organ system for dissecting these mechanisms.

Despite the elaborate structures decorated by pre-cuticle proteins, only mild defects in the vulva lumen shape have been detected in single mutants [20,48]. *let-653* loss had more dramatic effects when combined with chondroitin perturbations, again suggesting redundant contributions of multiple aECM factors to lumen shape [48].

3.5. The Pre-Cuticle Patterns the Cuticle

Towards the end of morphogenesis, once tissues have taken their shapes, pre-cuticle components disappear and are replaced by cuticle. How this transition occurs is not understood, but it is likely to be gradual rather than abrupt, with the pre-cuticle serving as a scaffold or template to which various collagens and other cuticle components are added. TEM imaging of discrete timepoints in the embryo suggested sequential addition of inner cuticle layers without obvious loss of outer layers [19], much as described for the eggshell [31]. Different cuticle collagens become expressed at different times during the molt cycle [87–89], so some could be present within both the pre-cuticle and the cuticle. When imaged directly, different pre-cuticle components disappear at different time points [48], suggesting gradual dismantling of the initial pre-cuticle structure. Consistent with a role in patterning the cuticle, many pre-cuticle mutants have compromised cuticle barrier functions, abnormal levels or exposure of cuticle surface lipids, and/or structural defects in cuticle alae ridges in larvae or adults [20,21,52,53].

4. Collagen-Based Cuticles and the Molt Cycle

The cuticles that line external epithelia of *C. elegans* larvae and adults are multi-layered structures composed of many different collagens and lipids, as well as other poorly characterized glycoproteins

and insoluble proteins collectively termed cuticulins (Figure 4) [17,90–92]. Cuticles attach to muscles to allow locomotion, provide a barrier to protect the organism from rupture, desiccation, and pathogens, and also shape (or maintain the shape of) tissues [93–100]. Between each larval stage, *C. elegans* molts into a new cuticle that is unique in structure and collagen composition for that life stage, but how these cuticles differ functionally is not clear [101,102]. Molting occurs four times, and then the adult cuticle remains present throughout the rest of the organism’s life (Figure 1) [18]. The expression of many genes rises and falls in accordance with distinct phases of the molt cycles [87,88,103,104], controlled by a molecular clock related to the circadian molecular clock of other organisms [105]. The molt process was recently extensively reviewed [18].

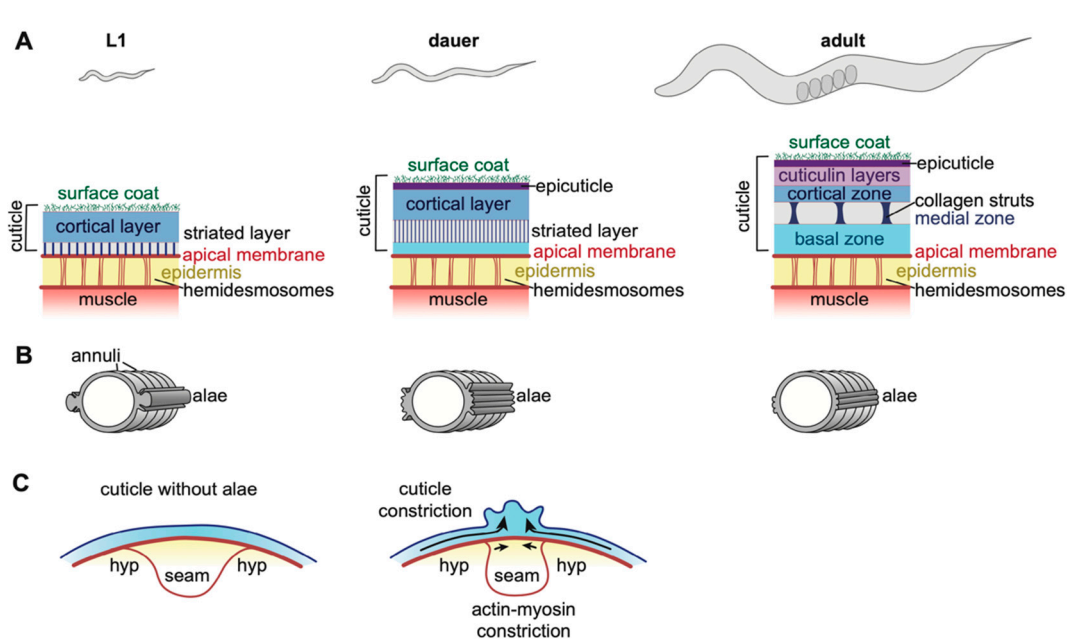


Figure 4. *C. elegans* epidermal cuticle. (A) Diagram of *C. elegans* at L1, dauer, and adult stages with cuticle structure at each stage (adapted from [106]). The epidermis connects the muscle and cuticle via hemidesmosomes. At the apical surface, the transmembrane proteins MUP-4 and MUA-3 link hemidesmosomes to the cuticle [55,57]. The cuticle is a multi-layered structure of collagens, cuticulins, lipids, and glycans [91,102,107]. The latter three are likely concentrated near the external surface of the cuticle, while collagens predominate in the basal zone and striated layers. Pre-cuticle and nascent cuticle may appear near the apical membrane prior to molts [53]. (B) Cross section of *C. elegans* at each stage indicating the position of alae and annuli. Furrows are the low points between annuli. Alae are not shown to scale. L1 larvae have one large alae ridge flanked by two smaller ones, adults have three alae ridges, while dauer larvae have five. (C) Model for alae formation. Constriction by actin-myosin in seam cells and by ZP proteins in the cuticle bend the cuticle into alae ridges [14,108].

4.1. Epidermal Cuticle Structure and Function

The epidermal cuticles have been the most intensively studied of all *C. elegans* aECMs [17,109]. A few dozen collagens and a smaller set of non-collagen protein components of this cuticle have been identified [110–112]. Most of the collagens are related to the mammalian FACIT (Fibril-Associated Collagens with Interrupted Triple helices) family, although some have unusual features not seen in mammalian collagens [110]. The *C. elegans* genome encodes > 170 members of this family, many of which presumably contribute to the cuticle (or pre-cuticle). The non-collagen cuticle components include several ZP domain proteins, lectins, and other unknown glycoproteins [90,91,93,113]. Finally, biochemical studies suggest that a variety of lipids are also present, including free fatty acids, phospholipids, triglycerides, and other more complex lipid types [107].

Cuticle components are organized into discrete layers (Figure 4A). Enzymatic digestion studies suggest that, in adults, collagens predominate in the basal-most striated layers, while cuticulins and other glycoproteins are present in the cortical and surface layers [102]. Glycosyltransferase (Bus) and nucleoside transporter (Srf) genes generate the glycoproteins of the outermost layer (Figure 4A) [93,95–97]. In adults, the basal and cortical zones are separated by an intermediate layer, which appears fluid-filled but contains connecting collagenous struts (Figure 4A). Mutants in the collagens BLI-1, 2, and 6 lack struts and have a Blistered (Bli) phenotype in which the cortical and basal layers of the cuticle detach from one another [102,114,115]. Beyond general categories, the specific contents of each cuticle layer are still little known.

One important function of the cuticle is to serve as a barrier against the penetration of toxins and other molecules. This barrier function is likely conferred by a lipid-rich layer that can be visualized by DiO/DiI staining or TEM (Figure 4A) [116,117]. Loss of enzymes that produce long-chain fatty acids (*pod-1*, *fasn-1*, *acs-20*) result in cuticle barrier defects, thinning of this lipid layer, and alae defects [94,118]. It remains unclear how lipids are secreted and incorporated into the cuticle, or if they are present in more than one layer. Interestingly, the transcription factor CEH-60 seems to act in the gut to affect cuticle barrier formation, suggesting that cuticle lipids may be derived from multiple tissue types [119].

The cuticle connects to the underlying epidermis via the matrilin-and fibrillin-related transmembrane proteins MUP-4 and MUA-3 [55–57]. It is not known which specific cuticle components are involved in binding these linkers, but annular furrow collagens (see below) are good candidates. The connection occurs at apical hemidesmosomes (Figure 4A), which contain the plectin VAB-10a and serve as attachment sites for cortical actin bundles, microtubules, and intermediate filaments [99,120]. Apical hemidesmosomes are in turn linked to basal hemidesmosomes via intermediate filaments, which span the epidermis [121]. Basal hemidesmosomes connect to the underlying body muscle via the transmembrane protein LET-805/myotactin [99,122]. Thus, the cuticle is anchored to both the epidermis and body muscle via the cytoskeleton. These attachments must be remodeled at each larval molt, but how this occurs and whether temporary attachments are formed is not known.

4.2. Alae and Annuli

Notable morphological features of epidermal cuticle are its two sets of cuticle ridges: annuli and alae (Figure 4B). Different cuticle components are responsible for building each of these features.

Annuli are circumferential ridges that are present at all stages (Figure 4B). The collagens DPY-2,3,7,8,10 are required to form annuli; of these, only DPY-7 and DPY-10 have been visualized, and both localize only at the low points or “furrows” of annuli, where the cuticle attaches to hemidesmosomes [123]. In contrast, the collagen DPY-13 is present on the raised portions of annuli [123]. Disruption of annuli triggers upregulated autophagy and hyperosmotic, detoxification, and innate immune responses in many tissues [124–126], indicating that one function of annuli is to sense and transmit information about cuticle damage.

Alae are longitudinal cuticle ridges that form above the lateral epidermis or “seam” cells (Figure 4B). They are present only in first stage (L1) larvae, dauer larvae, and adults and have distinct appearances at these different stages [17,101]. Several ZP proteins (CUT-1/3/5/6) localize to the alae of one or more stages, and are required to generate or shape them [14,90–92,113,127–129]. For example, CUT-1 promotes formation of dauer alae, CUT-3 promotes formation of L1 alae, and CUT-4 promotes formation of adult alae [14]. Both CUT-5 and the nidogen domain protein DEX-1 promote formation of alae in L1s and dauers, but not adults [14,130]. The collagens DPY-2, DPY-3, DPY-10 [123], DPY-5, DPY-11 and DPY-13 [124], and the secreted proline-rich-repeat protein MLT-10 [131] are all required for normal adult alae morphology; it’s not clear whether they are also required for development of L1 or dauer alae. Pre-cuticle components are also important for alae shaping [52,53,108,130]. Alae are thought to form by circumferential constriction of the seam epidermis and/or polymerization of membrane-proximal ZP matrix layers in cuticle or pre-cuticle, which leads to buckling of the overlying cuticle layers

(Figure 4C) [14,108]. The purpose of alae is not known, but two possible functions are to aid in locomotion or to serve as a reservoir of extra cuticle material to accommodate animal growth.

4.3. Epidermal Cuticles Maintain Body Length and Girth

Sidney Brenner's original genetic screens in *C. elegans* identified many body shape mutants that turned out to encode cuticle collagens [17,132,133]. The majority of these collagen mutants are notably short and fat (Dumpy; Dpy), while a smaller set are excessively long and thin (Long; Lon), develop cuticle delaminations (Blistered; Bli) or have twisted body axes (roller; Rol). Therefore, cuticle collagens can affect body shape in multiple ways.

The elongated worm shape of *C. elegans* arises through actomyosin-based constriction of the epidermis during embryogenesis with contributions from the pre-cuticular epidermal sheath (see above) [3,22,47,54,98,100]. Early studies of *sqt-3* cuticle collagen mutants (which are Dpy) revealed that this collagen was not needed for body elongation per se, but rather for maintenance of the elongated state [22]. This fits with the idea that most cuticle secretion happens after morphogenesis, and that tissue anchorage to the cuticle stabilizes the current shape established by the pre-cuticle.

Many matrix mutants that lack alae have shorter and wider seam cells and a shorter and wider body shape [14,123,124,130], suggesting that aECM factors that generate the alae also play a role in seam cell and body constriction.

The *C. elegans* TGF β signaling pathway affects body size, at least in part by regulating collagen gene expression. Mutants with reduced TGF β signaling have a small (Sma) body size despite normal cell numbers, while mutants with increased TGF β signaling are Lon [134–138]. These signaling mutants also have changes in intracellular lipid storage and in cuticle surface lipid accumulation [116,139,140]. Direct or indirect targets of TGF β -regulated Smad transcription factors include the collagen genes *rol-6*, *col-41*, *col-141*, and *col-142*, whose loss and/or overexpression also impacts body size [141]. Interestingly, mutations in some collagens also reduce expression levels of the TGF β ligand DBL-1, suggesting a positive feedback loop whereby cuticle structure maintains proper TGF β signaling [142]. Relationships between TGF β signaling and extracellular matrix organization also have been found in mammalian systems [143], and *C. elegans* could be a good system for understanding some of these connections.

4.4. Cuticles of Interfacial Tubes

Collagenous cuticles also line the interfacial tubes that connect the epidermis and the external environment to internal tissues (Figure 3F), but in most cases little is known regarding their specific composition. Since these tubes have somewhat different pre-cuticle components compared to the epidermis (Figure 3B,C, see above), it is possible that they also have distinct cuticle collagens or other components. These cuticles do have some unique morphological features. For example, electron micrographs show dramatic vertical striations within the cuticle of the buccal cavity [144] and orbital ridges surrounding the opening of the excretory pore [28]. The adult rectum is uniquely susceptible to bacterial adhesion and infection [145,146]; whether this is due to a unique cuticle makeup remains to be determined.

The most intensively studied interfacial tube cuticle has been that of the male rays. Rays are cuticle-lined glial tubules through which sensory neurites extend [147,148]. Cuticle proteins important for building the male rays include the ZP domain protein RAM-5 [149], the short, secreted peptide LON-8 [150], and the collagens RAM-2, COL-34, and SQT-1 [149,151]. Several proteins implicated in collagen processing are also required for male ray morphology, including the ADAMTS metalloprotease, ADT-1 [152], the collagen-modifying thioreductase DPY-11 [153,154], and the prolyl hydroxylase DPY-18 [151]. Tunicamycin treatment, which prevents glycosylation, results in severely deformed male rays with cuticular defects, indicating that glycoproteins are also directly or indirectly important for building the ray cuticle [155].

4.5. Regulation of the Molt Process

Molting involves the coordinated assembly and disassembly of pre-cuticles and cuticles. Many gene products are required for molting [156], including proteases [157–159], pre-cuticle [53] and cuticle components [131], endocytic proteins [160], metabolic enzymes [103,118,161], secretory pathway genes [69,162], and Hedgehog-and Patched-related genes [69,163]. The expression of many genes rises and falls in accordance with distinct phases of the molt cycle [87,88,103,104]. This process was recently extensively reviewed [18].

To secrete large amounts of cuticle proteins during molt, *C. elegans* coordinately alters secretory and stress pathways. Lysosome-related organelle (LRO) morphology changes dramatically in epidermal cells before and during ecdysis, indicating that LROs may be particularly important for molting [162]. In addition to their roles in protein and lipid degradation, these acidic vesicles are central hubs of the secretory pathway, that are able to send and receive cargo from endocytic, secretory, or lysosomal vesicles [164]. The high level of secretion presumably required to build a cuticle also relies on stress pathway regulation. Upregulation of ER stress proteins occurs in a developmentally regulated fashion during molting [165].

4.6. The Cuticle Changes during Aging

Degradation of the cuticle may be one major cause of aging-induced health decline. The adult *C. elegans* cuticle must remain intact throughout the organism's two weeks of adulthood, even as *C. elegans* continues to grow in both length and width. Over the course of one week of adulthood, cuticle structure becomes irregular and its stiffness declines [166]. Some cuticle collagens gradually decrease in expression level throughout adulthood, and excess expression of specific cuticle collagens throughout development can prolong life [167]. Food deprivation, pathogen infection, or other stressors also can trigger protective upregulation of collagen gene expression [167–170]. These observations suggest that cuticle degradation contributes to the aging process, but that the adult cuticle can be repaired when newly secreted aECM components are provided.

5. Chitin-Based Pharyngeal Cuticle

The pharynx, or foregut, is a myoepithelium with a cuticle that is different than the cuticle of the rest of the body. The pharyngeal cuticle contains the carbohydrate chitin [25], and may not contain collagen. It appears to contain different types of secreted matrix proteins, including pharynx-specific mucin-like proteins [171] and many proteins predicted to form amyloid (encoded by the *abu/pqn* paralog group genes) [87]. Consistent with the presence of amyloid, the pharyngeal cuticle stains with Congo Red, a marker for amyloid [87].

The pharynx transports bacteria through its lumen into its posterior end called the terminal bulb (TB). The TB contains teeth-like cuticular specializations in its grinder that break bacteria before passing them into the gut [26,27] (Figure 5A,B). The cuticle that lines the pharyngeal lumen and makes up the grinder is key to *C. elegans* feeding [172–174]. Loss of either chitin or the predicted amyloid-forming protein ABU-14 causes lumen shaping and/or grinder defects which results in poor transport and mashing of bacteria [25,87].

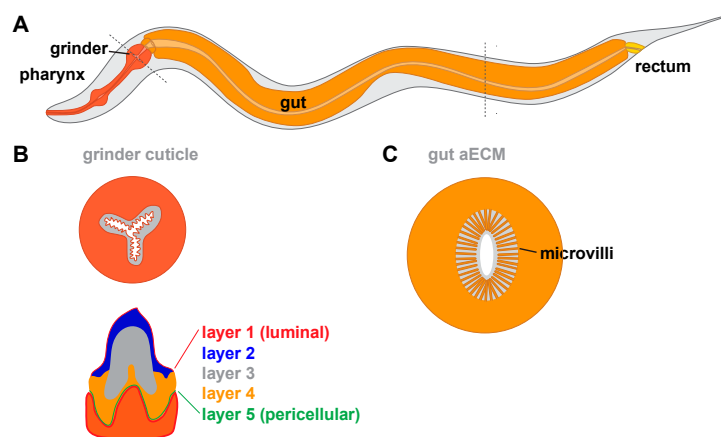


Figure 5. Tubes and aECMs of the *C. elegans* digestive tract. (A) Diagram of the digestive system. Different aECMs line the pharynx, gut and rectum. (B) Diagram of the pharyngeal grinder containing multiple teeth and the five observed aECM layers within a single tooth (adapted from [175]). Dark orange denotes pharyngeal cell cytoplasm. (C) Cross-section through the gut, showing apical microvilli surrounded by a membrane-proximal aECM (adapted from [176]). Light orange denotes intestinal cell cytoplasm.

Like the body cuticle, the pharyngeal cuticle is replaced with each larval molt cycle. However, in contrast to the body cuticle, which grows continuously, the pharyngeal cuticle grows only during the molt [87,177], perhaps due to the higher rigidity of this aECM. Following enzymatic digestion of the old cuticle, part of the old cuticle is expelled through the mouth, while the rest is swallowed [87,175]. There appears to be a pharyngeal pre-cuticle in the embryo [52], but its contents are largely uncharacterized, and it's not clear if it reappears during molt. Dedicated proteases, such as CPZ-1 [157], NAS-6, and NAS-7 [175,178], are required for pharyngeal cuticle removal during the molt.

Ultrastructural studies revealed that the pharyngeal grinder has five distinct layers that assemble in a sequential manner during molts (Figure 5B) [175]. It is not yet clear which molecular components are present in each layer. Interestingly, during grinder synthesis, pharyngeal muscle cells transiently lose their striated muscle-like appearance and take on a more epithelial and secretory, vesicle-filled, appearance, suggesting a toggling between the two aspects of their cell identity in order to build cuticle [175].

The pharyngeal cuticle has evolved specialized features in different nematodes. In the facultative predator nematode *Pristionchus pacificus*, the cuticle at the transition between the buccal cavity and the pharynx can take on two forms [179]. The first, stenostomatous, contains a single chitinous tooth, and is sufficient for ingesting bacteria. The second, predatory morph, eurystomatous, includes two teeth that can pierce the cuticles of other nematodes. The choice between these mouth-forms is made based on environmental inputs, including pheromones, diet, and habitat [179–182]. These factors converge on the neuronally-expressed sulfatase EUD-1 and the α -N-acetylglucosaminidases NAG-1 and NAG-2, which then activate chromatin modifiers to promote either the predatory morph or the bactericidal morph, respectively [183–185]. The *C. elegans* genome encodes several orthologs of *eud-1*, *nag-1*, and *nag-2* [186], but it is not known whether they impact cuticle or pharyngeal aECM structure.

6. aECMs of Internal Epithelia

Relatively little is known about the composition or functions of the non-cuticular aECMs that line *C. elegans* internal epithelia, such as those of the gut or uterus. However, these tissues do contain aECMs that likely play important roles in tissue shaping and/or function.

6.1. The Gut

The *C. elegans* gut is composed of sixteen ciliated cells lining a lumen [187]. Transmission electron microscopy (TEM) reveals that cilia are bathed in a ~1 micron thick electron-dense aECM from which bacteria appear to be excluded (Figure 5C) [176,188,189]. This membrane-proximal aECM layer resembles the mucin-rich glycocalyx of the mammalian gut [8]. Several secreted proteins can be detected within the larval gut lumen, including the lectins LEC-6 and LEC-10 [190], the leucine aminopeptidase LAP-1 [191], and the bacteria-killing lysozyme ILYS-3 [192]. The gene *f57f4.4*, which encodes a large secreted protein, is also expressed in the gut [193]. Future research is needed to determine whether these proteins contribute to the gut aECM, and to determine their roles in gut function.

6.2. The Uterus

The *C. elegans* uterus is a large, multicellular lumen into which fertilized eggs are deposited before passing through the vulva during egg laying. The uterus expands dramatically during L4 stage [194] and fills with an amorphous aECM visible by TEM (Figure 6). A set of secreted proteins and lipids are present in the uterus throughout adulthood (VIT-6, ULE-1–5) [29,195]. One of these, ULE-5, is deposited onto the surface of the eggshell, while the rest are retained within the uterine lumen and surround developing embryos [29]. Functions for these proteins are not described, and it is not clear whether these or other proteins are incorporated into the uterus aECM.

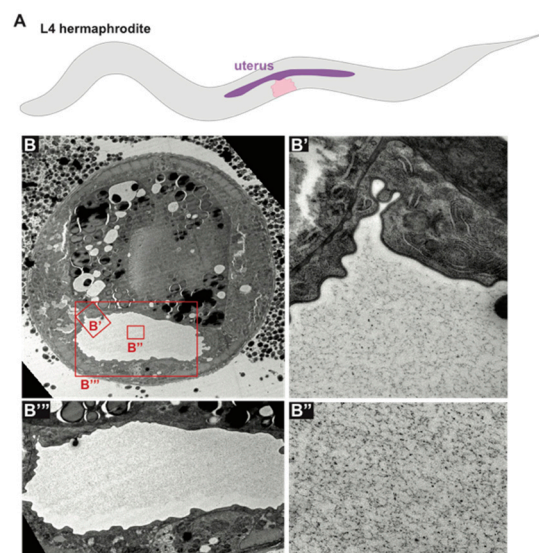


Figure 6. Uterine aECM. (A) Diagram of L4 stage *C. elegans* with vulva (pink) and expanded uterus (purple). (B) TEM of the uterus at mid-L4 stage. (B'–B''') The inflated uterine lumen is filled with a granular matrix of unknown composition. (Electron micrographs courtesy of Alessandro Sparacio).

6.3. The Excretory Canal Cell

The excretory canal cell extends four long lumenized tubules along the length of the worm, through which it is presumed to exchange osmolytes with the body cavity. It then drains its contents through the excretory duct and pore (Figure 3D) [61]. Although some electron micrographs show a meshwork within the canal lumens [21,28], the contents of this aECM are not known. At least one ZP protein, DYF-7, is expressed in the canal cell and may contribute to its aECM [49,52].

7. Outstanding Questions Regarding aECM

There remain many unanswered questions about how aECMs assemble, connect to underlying cells, and shape epithelia. aECMs are challenging to study as they generally do not develop fully in cell culture and can be destroyed by the fixation required to visualize aECMs in many animal systems.

C. elegans is an excellent model for addressing how aECMs assemble and function, as it offers a set of aECMs that can be visualized without fixation in vivo.

7.1. How Are aECM Components Trafficked to Apical Cell Surfaces?

Building an organized aECM requires that many different components are trafficked to the apical surface, and that matrix assembly occurs only once these components have arrived in their proper locations. We know little about the vesicular compartments through which most aECM proteins or lipids travel, or when or where these components become exposed to relevant conditions and partners for assembly into gels or fibrils. Studies of collagen-, mucin- or lipid-rich matrices in mammals have identified some specific vesicular compartments important for matrix delivery, but these compartments are not well understood, and whether *C. elegans* uses similar compartments is not yet known.

Collagens and other extracellular matrix cargos are thought to require extra-large vesicular or tubular compartments in order to traffic through the secretory system [196]. In *C. elegans*, as in other organisms, coat complex II (COPII) appears to be required for collagen secretion [197]. Recent studies in mammals have identified the transport and Golgi organization (TANGO1) protein as important for ER-to-Golgi trafficking of large proteins [198], but no TANGO1 ortholog has been identified in *C. elegans*. Instead, efficient secretion of at least some cuticle collagens requires the evolutionarily conserved ER protein TMEM131, which binds to the TRAPPC8 component of the Transfer Particle Protein III (TRAPIII) COPII-tethering complex [199].

In mammalian goblet cells of the lung and gut, large acidic vesicles deliver highly condensed mucin packets that expand once exposed to the higher pH of the extracellular environment [200]. Morphologically similar vesicles and spherically-expanding matrix packets have been seen by TEM within the vulF cells of the vulva [48]. The molecular nature of these vesicles is not known, but their cargo may include the ZP protein LET-653, which is capable of binding spherical aggregates in vitro [201].

In the mammalian lung, lamellar bodies process and deliver lipid-rich surfactant to alveolar air sacs [2]. *C. elegans* external epithelia likewise contain elaborate lamellar structures at their apical membranes [202–204]. RAL-1, a GTPase required for exosome secretion, and VHA-5, a component of the V-ATPase, associate with these stacks near the apical surface of seam cells and are required for alae formation [202,204]. These membrane stacks may therefore act as sites of secretory particle organization and/or biogenesis. Both apical membrane stacks and multi-vesicular bodies (MVBs) have been suggested to deliver hedgehog-like proteins and other cuticle components to the cuticle [202,204].

7.2. How Are aECMs Anchored to Cell Surfaces?

Many aECM components appear membrane-associated despite lacking obvious domains for membrane spanning or attachment, and in at least some cases, aECM-dependent tissue shaping involves effects on the cytoskeleton. Basal ECMs are generally thought to attach to cell surfaces and the cytoskeleton via integrins, whose extracellular face can bind ECM proteins and intracellular domains bind cytoskeleton modifiers [205]. In contrast, *C. elegans* body cuticles attach to the epidermis and hemidesmosomes via the transmembrane proteins MUP-4 [55] and MUA-3 [55]. It is unclear whether these or other unknown transmembrane proteins anchor other aECMs, such as the embryonic sheath or the pharyngeal cuticle, to apical membranes.

7.3. How Are aECMs Assembled and Disassembled?

C. elegans aECMs are highly dynamic and spatially specific, with many pre-cuticular aECM components present in restricted regions for mere hours before being replaced by cuticle [48,52]. Furthermore, aECMs can have dazzling complexity, with multiple layers composed of different aECM components [24,48,101,175]. The rapidity of development implies careful regulation of aECM assembly and disassembly by cell-type specific aECM anchors and proteases. However, how this occurs is almost entirely unknown.

aECMs also can be very large. For example, the mid-L4 vulva lumen expands to roughly 10 microns in diameter, with centrally located core aECM components located microns away from their originating cells [20,48]. Elaborate vesicle systems and molecular motors transport proteins to appropriate locations within cells [206], but it is not clear what mechanisms ensure proper placement of aECM proteins within a large extracellular compartment. Most models for aECM layer formation posit sequential rounds of local deposition and detachment [19,31,175], but other biophysical sorting mechanisms or luminal flows may facilitate the movement of some aECM proteins and lipids over longer distances.

7.4. What Is the Contribution of Individual aECM Components in Shaping Cell Surfaces?

Although mutant phenotypes for many individual aECM components have been described, the mechanisms by which those components shape their underlying cells often remain unclear. aECMs may shape cells directly by pushing or pulling on apical membranes or creating a stiff scaffold, or indirectly by modulating signaling or interacting with the cytoskeleton across the apical membrane. Identifying interactions between specific aECM proteins and understanding how they anchor to the apical membrane may shed light on how aECM components shape cells.

Many *C. elegans* aECM proteins are related to mammalian matrix proteins and therefore serve as suitable models for studying those specific protein families. For example, ZP proteins (including LET-653, NOAH-1, FBN-1 and CUT-1-6) are abundant in the *C. elegans* pre-cuticle or cuticle [14,20,47,50,91,113,128], and ZP proteins also are present within the mammalian egg coat and in or near aECMs of the gut, vascular and renal systems [207–212]. FBN-1 also is related to mammalian fibrillin, a component of mammalian stromal ECMs [213]. The *C. elegans* eLRRon family of pre-cuticle proteins (including LET-4, EGG-6 and SYM-1) [21,47] is related to the small leucine-rich proteoglycans (SLRPs) found in many mammalian ECMs [214]. Lipocalins are a family of known lipid transporters present in or near both *C. elegans* pre-cuticle and mammalian aECMs [53,62,63,215]. Finally, most *C. elegans* cuticle collagens are related to mammalian FACIT collagens. Further work on these proteins in the worm promises to shed light on the trafficking, assembly, and tissue-shaping properties of these conserved matrix protein families.

Funding: This work was funded by NIH grants R35 GM136315 to M.V.S. and T32 AR007465 to J.D.C.

Acknowledgments: We thank David Raizen and members of our laboratory for helpful discussions and comments on this manuscript, and Alessandro Sparacio for generating the TEM images used in Figure 6.

Conflicts of Interest: The authors declare no conflict of interest. The funders had no role in the design of the study; in the collection, analyses, or interpretation of data; in the writing of the manuscript, or in the decision to publish the results.

References

1. Luschnig, S.; Uv, A. Luminal matrices: An inside view on organ morphogenesis. *Exp. Cell Res.* **2014**, *321*, 64–70. [[CrossRef](#)] [[PubMed](#)]
2. Pérez-Gil, J. Structure of pulmonary surfactant membranes and films: The role of proteins and lipid-protein interactions. *Biochim. Biophys. Acta* **2008**, *1778*, 1676–1695. [[CrossRef](#)] [[PubMed](#)]
3. Tarbell, J.M.; Cancel, L.M. The glycocalyx and its significance in human medicine. *J. Intern. Med.* **2016**, *280*, 97–113. [[CrossRef](#)] [[PubMed](#)]
4. Walma, D.A.C.; Yamada, K.M. The extracellular matrix in development. *Development* **2020**, *147*. [[CrossRef](#)] [[PubMed](#)]
5. Jayadev, R.; Sherwood, D.R. Basement membranes. *Curr. Biol.* **2017**, *27*, R207–R211. [[CrossRef](#)] [[PubMed](#)]
6. Bernhard, W. Lung surfactant: Function and composition in the context of development and respiratory physiology. *Ann. Anat.* **2016**, *208*, 146–150. [[CrossRef](#)] [[PubMed](#)]
7. Gaudette, S.; Hughes, D.; Boller, M. The endothelial glycocalyx: Structure and function in health and critical illness. *J. Vet. Emerg. Crit. Care (San Antonio)* **2020**. [[CrossRef](#)]

8. Johansson, M.E.; Ambort, D.; Pelaseyed, T.; Schutte, A.; Gustafsson, J.K.; Ermund, A.; Hansson, G.C. Composition and functional role of the mucus layers in the intestine. *Cell. Mol. Life Sci.* **2011**, *68*, 3635–3641. [[CrossRef](#)]
9. Bhattacharya, N.; Sato, W.J.; Kelly, A.; Ganguli-Indra, G.; Indra, A.K. Epidermal Lipids: Key Mediators of Atopic Dermatitis Pathogenesis. *Trends Mol. Med.* **2019**, *25*, 551–562. [[CrossRef](#)]
10. Dartt, D.A. Tear lipocalin: Structure and function. *Ocul. Surf.* **2011**, *9*, 126–138. [[CrossRef](#)]
11. Devine, W.P.; Lubarsky, B.; Shaw, K.; Luschnig, S.; Messina, L.; Krasnow, M.A. Requirement for chitin biosynthesis in epithelial tube morphogenesis. *Proc. Natl. Acad. Sci. USA* **2005**, *102*, 17014–17019. [[CrossRef](#)] [[PubMed](#)]
12. Fernandes, I.; Chanut-Delalande, H.; Ferrer, P.; Latapie, Y.; Waltzer, L.; Affolter, M.; Plaza, S. Zona pellucida domain proteins remodel the apical compartment for localized cell shape changes. *Dev. Cell* **2010**, *18*, 64–76. [[CrossRef](#)] [[PubMed](#)]
13. Plaza, S.; Chanut-Delalande, H.; Fernandes, I.; Wassarman, P.M.; Payre, F. From A to Z: Apical structures and zona pellucida-domain proteins. *Trends Cell Biol.* **2010**, *20*, 524–532. [[CrossRef](#)]
14. Sapiro, M.R.; Hilliard, M.A.; Cermola, M.; Favre, R.; Bazzicalupo, P. The Zona Pellucida domain containing proteins, CUT-1, CUT-3 and CUT-5, play essential roles in the development of the larval alae in *Caenorhabditis elegans*. *Dev. Biol.* **2005**, *282*, 231–245. [[CrossRef](#)] [[PubMed](#)]
15. Chappell, D.; Jacob, M.; Paul, O.; Rehm, M.; Welsch, U.; Stoeckelhuber, M.; Becker, B.F. The glycocalyx of the human umbilical vein endothelial cell: An impressive structure ex vivo but not in culture. *Circ. Res.* **2009**, *104*, 1313–1317. [[CrossRef](#)]
16. Corsi, A.K.; Wightman, B.; Chalfie, M. A Transparent window into biology: A primer on *Caenorhabditis elegans*. *WormBook* **2015**, 1–31. [[CrossRef](#)]
17. Page, A.P.; Johnstone, I.L. The cuticle. *WormBook* **2007**, 1–15. [[CrossRef](#)]
18. Lazetic, V.; Fay, D.S. Molting in *C. elegans*. *Worm* **2017**, *6*, e1330246. [[CrossRef](#)]
19. Costa, M.; Draper, B.W.; Priess, J.R. The role of actin filaments in patterning the *Caenorhabditis elegans* cuticle. *Dev. Biol.* **1997**, *184*, 373–384. [[CrossRef](#)]
20. Gill, H.K.; Cohen, J.D.; Ayala-Figueroa, J.; Forman-Rubinsky, R.; Poggioli, C.; Bickard, K.; Sundaram, M.V. Integrity of Narrow Epithelial Tubes in the *C. elegans* Excretory System Requires a Transient Luminal Matrix. *PLoS Genet.* **2016**, *12*, e1006205. [[CrossRef](#)]
21. Mancuso, V.P.; Parry, J.M.; Storer, L.; Poggioli, C.; Nguyen, K.C.; Hall, D.H.; Sundaram, M.V. Extracellular leucine-rich repeat proteins are required to organize the apical extracellular matrix and maintain epithelial junction integrity in *C. elegans*. *Development* **2012**, *139*, 979–990. [[CrossRef](#)] [[PubMed](#)]
22. Priess, J.R.; Hirsh, D.I. *Caenorhabditis elegans* morphogenesis: The role of the cytoskeleton in elongation of the embryo. *Dev. Biol.* **1986**, *117*, 156–173. [[CrossRef](#)]
23. Olson, S.K.; Bishop, J.R.; Yates, J.R.; Oegema, K.; Esko, J.D. Identification of novel chondroitin proteoglycans in *Caenorhabditis elegans*: Embryonic cell division depends on CPG-1 and CPG-2. *J. Cell Biol.* **2006**, *173*, 985–994. [[CrossRef](#)] [[PubMed](#)]
24. Stein, K.K.; Golden, A. The *C. elegans* eggshell. *WormBook* **2018**, *2018*, 1–36. [[CrossRef](#)] [[PubMed](#)]
25. Zhang, Y.; Foster, J.M.; Nelson, L.S.; Ma, D.; Carlow, C.K. The chitin synthase genes *chs-1* and *chs-2* are essential for *C. elegans* development and responsible for chitin deposition in the eggshell and pharynx, respectively. *Dev. Biol.* **2005**, *285*, 330–339. [[CrossRef](#)]
26. Albertson, D.G.; Thomson, J.N. The pharynx of *Caenorhabditis elegans*. *Philos. Trans. R. Soc. B Biol. Sci.* **1976**, *275*, 299–325. [[CrossRef](#)]
27. Mango, S.E. The *C. elegans* pharynx: A model for organogenesis. *WormBook* **2007**, 1–26. [[CrossRef](#)]
28. Altun, Z.F.; Herndon, L.A.; Wolkow, C.A.; Crocker, C.; Lints, R.; Hall, D.H. (2002–2020). WormAtlas. Available online: <http://www.wormatlas.org> (accessed on 3 July 2020).
29. Zimmerman, S.M.; Hinkson, I.V.; Elias, J.E.; Kim, S.K. Reproductive Aging Drives Protein Accumulation in the Uterus and Limits Lifespan in *C. elegans*. *PLoS Genet.* **2015**, *11*, e1005725. [[CrossRef](#)]
30. Gonzalez, D.P.; Lamb, H.V.; Partida, D.; Wilson, Z.T.; Harrison, M.C.; Prieto, J.A.; Olson, S.K. CBD-1 organizes two independent complexes required for eggshell vitelline layer formation and egg activation in *C. elegans*. *Dev. Biol.* **2018**, *442*, 288–300. [[CrossRef](#)]
31. Olson, S.K.; Greenan, G.; Desai, A.; Muller-Reichert, T.; Oegema, K. Hierarchical assembly of the eggshell and permeability barrier in *C. elegans*. *J. Cell Biol.* **2012**, *198*, 731–748. [[CrossRef](#)]

32. Johnston, W.L.; Krizus, A.; Dennis, J.W. The eggshell is required for meiotic fidelity, polar-body extrusion and polarization of the *C. elegans* embryo. *BMC Biol.* **2006**, *4*, 35. [[CrossRef](#)] [[PubMed](#)]
33. Starich, T.A.; Greenstein, D. Gap junctions deliver malonyl-CoA from soma to germline to support embryogenesis in *Caenorhabditis elegans*. *Elife* **2020**, *9*, e58619. [[CrossRef](#)] [[PubMed](#)]
34. Rappleye, C.A.; Paredes, A.R.; Smith, C.W.; McDonald, K.L.; Aroian, R.V. The coronin-like protein POD-1 is required for anterior-posterior axis formation and cellular architecture in the nematode *Caenorhabditis elegans*. *Genes Dev.* **1999**, *13*, 2838–2851. [[CrossRef](#)] [[PubMed](#)]
35. Bai, X.; Huang, L.-J.; Chen, S.-W.; Nebenfuhr, B.; Wysolmerski, B.; Wu, J.-C.; Wang, C.-W. Loss of the seipin gene perturbs eggshell formation in *C. elegans*. *Development* **2020**. [[CrossRef](#)]
36. Litscher, E.S.; Wassarman, P.M. Evolution, structure, and synthesis of vertebrate egg-coat proteins. *Trends Dev. Biol.* **2014**, *8*, 65–76. [[PubMed](#)]
37. Krenger, R.; Burri, J.T.; Lehnert, T.; Nelson, B.J.; Gijs, M.A.M. Force microscopy of the *Caenorhabditis elegans* embryonic eggshell. *Microsyst. Nanoeng.* **2020**, *6*, 29. [[CrossRef](#)]
38. Edgar, L.G.; McGhee, J.D. DNA synthesis and the control of embryonic gene expression in *C. elegans*. *Cell* **1988**, *53*, 589–599. [[CrossRef](#)]
39. Johnston, W.L.; Dennis, J.W. The eggshell in the *C. elegans* oocyte-to-embryo transition. *Genesis* **2012**, *50*, 333–349. [[CrossRef](#)]
40. Parry, J.M.; Velarde, N.V.; Lefkovith, A.J.; Zegarek, M.H.; Hang, J.S.; Ohm, J.; Singson, A. EGG-4 and EGG-5 Link Events of the Oocyte-to-Embryo Transition with Meiotic Progression in *C. elegans*. *Curr. Biol.* **2009**, *19*, 1752–1757. [[CrossRef](#)]
41. Rappleye, C.A.; Tagawa, A.; Le Bot, N.; Ahringer, J.; Aroian, R.V. Involvement of fatty acid pathways and cortical interaction of the pronuclear complex in *Caenorhabditis elegans* embryonic polarity. *BMC Dev. Biol.* **2003**, *3*, 8. [[CrossRef](#)]
42. Rappleye, C.A.; Tagawa, A.; Lyczak, R.; Bowerman, B.; Aroian, R.V. The anaphase-promoting complex and separin are required for embryonic anterior-posterior axis formation. *Dev. Cell* **2002**, *2*, 195–206. [[CrossRef](#)]
43. Laufer, J.S.; Bazzicalupo, P.; Wood, W.B. Segregation of developmental potential in early embryos of *Caenorhabditis elegans*. *Cell* **1980**, *19*, 569–577. [[CrossRef](#)]
44. Schierenberg, E. Reversal of cellular polarity and early cell-cell interaction in the embryos of *Caenorhabditis elegans*. *Dev. Biol.* **1987**, *122*, 452–463. [[CrossRef](#)]
45. Wood, W.B.; Bergmann, D.; Florance, A. Maternal effect of low temperature on handedness determination in *C. elegans* embryos. *Dev. Genet.* **1996**, *19*, 222–230. [[CrossRef](#)]
46. Schierenberg, E.; Junkersdorf, B. The role of eggshell and underlying vitelline membrane for normal pattern formation in the early *C. elegans* embryo. *Roux Arch. Dev. Biol.* **1992**, *202*, 10–16. [[CrossRef](#)] [[PubMed](#)]
47. Vuong-Brender, T.T.K.; Suman, S.K.; Labouesse, M. The apical ECM preserves embryonic integrity and distributes mechanical stress during morphogenesis. *Development* **2017**, *144*, 4336–4349. [[CrossRef](#)] [[PubMed](#)]
48. Cohen, J.D.; Sparacio, A.P.; Belfi, A.C.; Forman-Rubinsky, R.; Hall, D.H.; Maul-Newby, H.; Sundaram, M.V. A multi-layered and dynamic apical extracellular matrix shapes the vulva lumen in *Caenorhabditis elegans*. *Elife* **2020**, *9*, e57874. [[CrossRef](#)] [[PubMed](#)]
49. Heiman, M.G.; Shaham, S. DEX-1 and DYF-7 establish sensory dendrite length by anchoring dendritic tips during cell migration. *Cell* **2009**, *137*, 344–355. [[CrossRef](#)]
50. Kelley, M.; Yochem, J.; Krieg, M.; Calixto, A.; Heiman, M.G.; Kuzmanov, A.; Fay, D.S. FBN-1, a fibrillin-related protein, is required for resistance of the epidermis to mechanical deformation during *C. elegans* embryogenesis. *Elife* **2015**, *4*. [[CrossRef](#)]
51. Low, I.I.C.; Williams, C.R.; Chong, M.K.; McLachlan, I.G.; Wierbowski, B.M.; Kolotuev, I.; Heiman, M.G. Morphogenesis of neurons and glia within an epithelium. *Development* **2019**, *146*. [[CrossRef](#)]
52. Cohen, J.D.; Flatt, K.M.; Schroeder, N.E.; Sundaram, M.V. Epithelial Shaping by Diverse Apical Extracellular Matrices Requires the Nidogen Domain Protein DEX-1 in *Caenorhabditis elegans*. *Genetics* **2019**, *211*, 185–200. [[CrossRef](#)] [[PubMed](#)]
53. Forman-Rubinsky, R.; Cohen, J.D.; Sundaram, M.V. Lipocalins Are Required for Apical Extracellular Matrix Organization and Remodeling in *Caenorhabditis elegans*. *Genetics* **2017**, *207*, 625–642. [[CrossRef](#)] [[PubMed](#)]
54. Vuong-Brender, T.T.K.; Ben Amar, M.; Pontabry, J.; Labouesse, M. The interplay of stiffness and force anisotropies drives embryo elongation. *Elife* **2017**, *6*. [[CrossRef](#)] [[PubMed](#)]

55. Bercher, M.; Wahl, J.; Vogel, B.E.; Lu, C.; Hedgecock, E.M.; Hall, D.H.; Plenefisch, J.D. mua-3, a gene required for mechanical tissue integrity in *Caenorhabditis elegans*, encodes a novel transmembrane protein of epithelial attachment complexes. *J. Cell Biol.* **2001**, *154*, 415–426. [[CrossRef](#)]
56. Fotopoulos, P.; Kim, J.; Hyun, M.; Qamari, W.; Lee, I.; You, Y.J. DPY-17 and MUA-3 Interact for Connective Tissue-Like Tissue Integrity in *Caenorhabditis elegans*: A Model for Marfan Syndrome. *G3 (Bethesda)* **2015**, *5*, 1371–1378. [[CrossRef](#)]
57. Hong, L.; Elbl, T.; Ward, J.; Franzini-Armstrong, C.; Rybicka, K.K.; Gatewood, B.K.; Bucher, E.A. MUP-4 is a novel transmembrane protein with functions in epithelial cell adhesion in *Caenorhabditis elegans*. *J. Cell Biol.* **2001**, *154*, 403–414. [[CrossRef](#)]
58. Bokhove, M.; Jovine, L. Structure of Zona Pellucida Module Proteins. *Curr. Top. Dev. Biol.* **2018**, *130*, 413–442. [[CrossRef](#)]
59. Davies, A.G.; Spike, C.A.; Shaw, J.E.; Herman, R.K. Functional overlap between the mec-8 gene and five sym genes in *Caenorhabditis elegans*. *Genetics* **1999**, *153*, 117–134.
60. Nelson, F.K.; Albert, P.S.; Riddle, D.L. Fine structure of the *Caenorhabditis elegans* secretory-excretory system. *J. Ultrastruct. Res.* **1983**, *82*, 156–171. [[CrossRef](#)]
61. Sundaram, M.V.; Buechner, M. The *Caenorhabditis elegans* Excretory System: A Model for Tubulogenesis, Cell Fate Specification, and Plasticity. *Genetics* **2016**, *203*, 35–63. [[CrossRef](#)]
62. Pu, P.; Stone, C.E.; Burdick, J.T.; Murray, J.I.; Sundaram, M.V. The Lipocalin LPR-1 Cooperates with LIN-3/EGF Signaling To Maintain Narrow Tube Integrity in *Caenorhabditis elegans*. *Genetics* **2017**, *205*, 1247–1260. [[CrossRef](#)] [[PubMed](#)]
63. Stone, C.E.; Hall, D.H.; Sundaram, M.V. Lipocalin signaling controls unicellular tube development in the *Caenorhabditis elegans* excretory system. *Dev. Biol.* **2009**, *329*, 201–211. [[CrossRef](#)] [[PubMed](#)]
64. Fan, L.; Kovacevic, I.; Heiman, M.G.; Bao, Z. A multicellular rosette-mediated collective dendrite extension. *Elife* **2019**, *8*. [[CrossRef](#)] [[PubMed](#)]
65. Grimbert, S.; Mastronardi, K.; Christensen, R.; Law, C.; Fay, D.; Piekny, A. Multi-tissue patterning drives anterior morphogenesis of the *C. elegans* embryo. *bioRxiv* **2020**. [[CrossRef](#)]
66. Oikonomou, G.; Shaham, S. The glia of *Caenorhabditis elegans*. *Glia* **2011**, *59*, 1253–1263. [[CrossRef](#)]
67. Yochem, J.; Bell, L.R.; Herman, R.K. The identities of sym-2, sym-3 and sym-4, three genes that are synthetically lethal with mec-8 in *Caenorhabditis elegans*. *Genetics* **2004**, *168*, 1293–1306. [[CrossRef](#)]
68. Schouteden, C.; Serwas, D.; Palfy, M.; Dammermann, A. The ciliary transition zone functions in cell adhesion but is dispensable for axoneme assembly in *C. elegans*. *J. Cell Biol.* **2015**, *210*, 35–44. [[CrossRef](#)] [[PubMed](#)]
69. Michaux, G.; Gansmuller, A.; Hindelang, C.; Labouesse, M. CHE-14, a protein with a sterol-sensing domain, is required for apical sorting in *C. elegans* ectodermal epithelial cells. *Curr. Biol.* **2000**, *10*, 1098–1107. [[CrossRef](#)]
70. Oikonomou, G.; Perens, E.A.; Lu, Y.; Shaham, S. Some, but not all, retromer components promote morphogenesis of *C. elegans* sensory compartments. *Dev. Biol.* **2012**, *362*, 42–49. [[CrossRef](#)]
71. Oikonomou, G.; Perens, E.A.; Lu, Y.; Watanabe, S.; Jorgensen, E.M.; Shaham, S. Opposing activities of LIT-1/NLK and DAF-6/patched-related direct sensory compartment morphogenesis in *C. elegans*. *PLoS Biol.* **2011**, *9*, e1001121. [[CrossRef](#)]
72. Perens, E.A.; Shaham, S. *C. elegans* daf-6 encodes a patched-related protein required for lumen formation. *Dev. Cell* **2005**, *8*, 893–906. [[CrossRef](#)] [[PubMed](#)]
73. Singhal, A.; Shaham, S. Infrared laser-induced gene expression for tracking development and function of single *C. elegans* embryonic neurons. *Nat. Commun.* **2017**, *8*, 14100. [[CrossRef](#)] [[PubMed](#)]
74. Hong, H.; Chen, H.; Zhang, Y.; Wu, Z.; Zhang, Y.; Zhang, Y.; Wei, Q. An extracellular protein regulates patched-related/DAF-6-mediated sensory compartment formation in *C. elegans*. *bioRxiv* **2020**. [[CrossRef](#)]
75. Gupta, B.P.; Hanna-Rose, W.; Sternberg, P.W. Morphogenesis of the vulva and the vulval-uterine connection. *WormBook* **2012**, 1–20. [[CrossRef](#)]
76. Sternberg, P.W.; Horvitz, H.R. The combined action of two intercellular signaling pathways specifies three cell fates during vulval induction in *C. elegans*. *Cell* **1989**, *58*, 679–693. [[CrossRef](#)]
77. Farooqui, S.; Pellegrino, M.W.; Rimann, I.; Morf, M.K.; Müller, L.; Fröhli, E.; Hajnal, A. Coordinated lumen contraction and expansion during vulval tube morphogenesis in *Caenorhabditis elegans*. *Dev. Cell* **2012**, *23*, 494–506. [[CrossRef](#)]

78. Hwang, H.Y.; Horvitz, H.R. The *Caenorhabditis elegans* vulval morphogenesis gene *sqv-4* encodes a UDP-glucose dehydrogenase that is temporally and spatially regulated. *Proc. Natl. Acad. Sci. USA* **2002**, *99*, 14224–14229. [[CrossRef](#)]
79. Hwang, H.Y.; Horvitz, H.R. The SQV-1 UDP-glucuronic acid decarboxylase and the SQV-7 nucleotide-sugar transporter may act in the Golgi apparatus to affect *Caenorhabditis elegans* vulval morphogenesis and embryonic development. *Proc. Natl. Acad. Sci. USA* **2002**, *99*, 14218–14223. [[CrossRef](#)]
80. Hwang, H.Y.; Olson, S.K.; Brown, J.R.; Esko, J.D.; Horvitz, H.R. The *Caenorhabditis elegans* genes *sqv-2* and *sqv-6*, which are required for vulval morphogenesis, encode glycosaminoglycan galactosyltransferase II and xylosyltransferase. *J. Biol. Chem.* **2003**, *278*, 11735–11738. [[CrossRef](#)]
81. Hwang, H.Y.; Olson, S.K.; Esko, J.D.; Horvitz, H.R. *Caenorhabditis elegans* early embryogenesis and vulval morphogenesis require chondroitin biosynthesis. *Nature* **2003**, *423*, 439–443. [[CrossRef](#)]
82. Yang, Q.; Roiz, D.; Mereu, L.; Daube, M.; Hajnal, A. The Invading Anchor Cell Induces Lateral Membrane Constriction during Vulval Lumen Morphogenesis in *C. elegans*. *Dev. Cell* **2017**, *42*, 271–285.e273. [[CrossRef](#)] [[PubMed](#)]
83. Mok, D.Z.; Sternberg, P.W.; Inoue, T. Morphologically defined sub-stages of *C. elegans* vulval development in the fourth larval stage. *BMC Dev. Biol.* **2015**, *15*, 26. [[CrossRef](#)] [[PubMed](#)]
84. Herman, T.; Hartweg, E.; Horvitz, H.R. *sqv* mutants of *Caenorhabditis elegans* are defective in vulval epithelial invagination. *Proc. Natl. Acad. Sci. USA* **1999**, *96*, 968–973. [[CrossRef](#)] [[PubMed](#)]
85. Suzuki, N.; Toyoda, H.; Sano, M.; Nishiwaki, K. Chondroitin acts in the guidance of gonadal distal tip cells in *C. elegans*. *Dev. Biol.* **2006**, *300*, 635–646. [[CrossRef](#)]
86. Noborn, F.; Gomez Toledo, A.; Nasir, W.; Nilsson, J.; Dierker, T.; Kjellén, L.; Larson, G. Expanding the chondroitin glycoproteome of *Caenorhabditis elegans*. *J. Biol. Chem.* **2018**, *293*, 379–389. [[CrossRef](#)]
87. George-Raizen, J.B.; Shockley, K.R.; Trojanowski, N.F.; Lamb, A.L.; Raizen, D.M. Dynamically-expressed prion-like proteins form a cuticle in the pharynx of *Caenorhabditis elegans*. *Biol. Open* **2014**, *3*, 1139–1149. [[CrossRef](#)]
88. Hendriks, G.J.; Gaidatzis, D.; Aeschmann, F.; Großhans, H. Extensive oscillatory gene expression during *C. elegans* larval development. *Mol. Cell* **2014**, *53*, 380–392. [[CrossRef](#)]
89. Johnstone, I.L.; Barry, J.D. Temporal reiteration of a precise gene expression pattern during nematode development. *EMBO J.* **1996**, *15*, 3633–3639. [[CrossRef](#)]
90. Favre, R.; Cermola, M.; Nunes, C.P.; Hermann, R.; Muller, M.; Bazzicalupo, P. Immuno-cross-reactivity of CUT-1 and cuticlin epitopes between *Ascaris lumbricoides*, *Caenorhabditis elegans*, and *Heterorhabditis*. *J. Struct. Biol.* **1998**, *123*, 1–7. [[CrossRef](#)]
91. Favre, R.; Hermann, R.; Cermola, M.; Hohenberg, H.; Muller, M.; Bazzicalupo, P. Immuno-gold-labelling of CUT-1, CUT-2 and cuticlin epitopes in *Caenorhabditis elegans* and *Heterorhabditis* sp. processed by high pressure freezing and freeze-substitution. *J. Submicrosc. Cytol. Pathol.* **1995**, *27*, 341–347.
92. Lewis, E.; Hunter, S.J.; Tetley, L.; Nunes, C.P.; Bazzicalupo, P.; Devaney, E. *cut-1*-like genes are present in the filarial nematodes, *Brugia pahangi* and *Brugia malayi*, and, as in other nematodes, code for components of the cuticle. *Mol. Biochem. Parasitol.* **1999**, *101*, 173–183. [[CrossRef](#)]
93. Gravato-Nobre, M.J.; Stroud, D.; O'Rourke, D.; Darby, C.; Hodgkin, J. Glycosylation genes expressed in seam cells determine complex surface properties and bacterial adhesion to the cuticle of *Caenorhabditis elegans*. *Genetics* **2011**, *187*, 141–155. [[CrossRef](#)] [[PubMed](#)]
94. Kage-Nakadai, E.; Kobuna, H.; Kimura, M.; Gengyo-Ando, K.; Inoue, T.; Arai, H.; Mitani, S. Two very long chain fatty acid acyl-CoA synthetase genes, *acs-20* and *acs-22*, have roles in the cuticle surface barrier in *Caenorhabditis elegans*. *PLoS ONE* **2010**, *5*, e8857. [[CrossRef](#)] [[PubMed](#)]
95. Palaima, E.; Leymarie, N.; Stroud, D.; Mizanur, R.M.; Hodgkin, J.; Gravato-Nobre, M.J.; Cipollo, J.F. The *Caenorhabditis elegans* *bus-2* mutant reveals a new class of O-glycans affecting bacterial resistance. *J. Biol. Chem.* **2010**, *285*, 17662–17672. [[CrossRef](#)]
96. Parsons, L.M.; Mizanur, R.M.; Jankowska, E.; Hodgkin, J.; O'Rourke, D.; Stroud, D.; Cipollo, J.F. *Caenorhabditis elegans* bacterial pathogen resistant *bus-4* mutants produce altered mucins. *PLoS ONE* **2014**, *9*, e107250. [[CrossRef](#)]
97. Partridge, F.A.; Tearle, A.W.; Gravato-Nobre, M.J.; Schafer, W.R.; Hodgkin, J. The *C. elegans* glycosyltransferase BUS-8 has two distinct and essential roles in epidermal morphogenesis. *Dev. Biol.* **2008**, *317*, 549–559. [[CrossRef](#)]

98. Quintin, S.; Wang, S.; Pontabry, J.; Bender, A.; Robin, F.; Hyenne, V.; Labouesse, M. Non-centrosomal epidermal microtubules act in parallel to LET-502/ROCK to promote *C. elegans* elongation. *Development* **2016**, *143*, 160–173. [[CrossRef](#)]
99. Suman, S.K.; Daday, C.; Ferraro, T.; Vuong-Brender, T.; Tak, S.; Quintin, S.; Labouesse, M. The plakin domain of *C. elegans* VAB-10/plectin acts as a hub in a mechanotransduction pathway to promote morphogenesis. *Development* **2019**, *146*. [[CrossRef](#)]
100. Zhang, H.; Landmann, F.; Zahreddine, H.; Rodriguez, D.; Koch, M.; Labouesse, M. A tension-induced mechanotransduction pathway promotes epithelial morphogenesis. *Nature* **2011**, *471*, 99–103. [[CrossRef](#)]
101. Cox, G.N.; Kusch, M.; DeNevi, K.; Edgar, R.S. Temporal regulation of cuticle synthesis during development of *Caenorhabditis elegans*. *Dev. Biol.* **1981**, *84*, 277–285. [[CrossRef](#)]
102. Cox, G.N.; Kusch, M.; Edgar, R.S. Cuticle of *Caenorhabditis elegans*: Its isolation and partial characterization. *J. Cell Biol.* **1981**, *90*, 7–17. [[CrossRef](#)] [[PubMed](#)]
103. Feng, L.; Shou, Q.; Butcher, R.A. Identification of a dTDP-rhamnose biosynthetic pathway that oscillates with the molting cycle in *Caenorhabditis elegans*. *Biochem. J.* **2016**, *473*, 1507–1521. [[CrossRef](#)] [[PubMed](#)]
104. Turek, M.; Bringmann, H. Gene expression changes of *Caenorhabditis elegans* larvae during molting and sleep-like lethargus. *PLoS ONE* **2014**, *9*, e113269. [[CrossRef](#)] [[PubMed](#)]
105. Monsalve, G.C.; Van Buskirk, C.; Frand, A.R. LIN-42/PERIOD controls cyclical and developmental progression of *C. elegans* molts. *Curr. Biol.* **2011**, *21*, 2033–2045. [[CrossRef](#)] [[PubMed](#)]
106. Cox, G.N.; Staprans, S.; Edgar, R.S. The cuticle of *Caenorhabditis elegans*. II. Stage-specific changes in ultrastructure and protein composition during postembryonic development. *Dev. Biol.* **1981**, *86*, 456–470. [[CrossRef](#)]
107. Blaxter, M.L. Cuticle surface proteins of wild type and mutant *Caenorhabditis elegans*. *J. Biol. Chem.* **1993**, *268*, 6600–6609.
108. Katz, S.S.; Maybrun, C.; Maul-Newby, H.M.; Frand, A.R. Non-canonical apical constriction shapes emergent matrices in *C. elegans*. *bioRxiv* **2018**, 189951. [[CrossRef](#)]
109. Chisholm, A.D.; Xu, S. The *Caenorhabditis elegans* epidermis as a model skin. II: Differentiation and physiological roles. *Wiley Interdiscip. Rev. Dev. Biol.* **2012**, *1*, 879–902. [[CrossRef](#)]
110. Johnstone, I.L. Cuticle collagen genes. Expression in *Caenorhabditis elegans*. *Trends Genet.* **2000**, *16*, 21–27. [[CrossRef](#)]
111. Kramer, J.M.; Cox, G.N.; Hirsh, D. Expression of the *Caenorhabditis elegans* collagen genes col-1 and col-2 is developmentally regulated. *J. Biol. Chem.* **1985**, *260*, 1945–1951.
112. Thein, M.C.; McCormack, G.; Winter, A.D.; Johnstone, I.L.; Shoemaker, C.B.; Page, A.P. *Caenorhabditis elegans* exoskeleton collagen COL-19: An adult-specific marker for collagen modification and assembly, and the analysis of organismal morphology. *Dev. Dyn.* **2003**, *226*, 523–539. [[CrossRef](#)] [[PubMed](#)]
113. Ristoratore, F.; Cermola, M.; Nola, M.; Bazzicalupo, P.; Favre, R. Ultrastructural immuno-localization of CUT-1 and CUT-2 antigenic sites in the cuticles of the nematode *Caenorhabditis elegans*. *J. Submicrosc. Cytol. Pathol.* **1994**, *26*, 437–443. [[PubMed](#)]
114. de Melo, J.V.; de Souza, W.; Peixoto, C.A. Ultrastructural analyses of the *Caenorhabditis elegans* DR 847 bli-1(n361) mutant which produces abnormal cuticle blisters. *J. Submicrosc. Cytol. Pathol.* **2002**, *34*, 291–297. [[PubMed](#)]
115. de Melo, J.V.; de Souza, W.; Peixoto, C.A. Immunocytochemical and freeze-fracture characterization of the *Caenorhabditis elegans* DR 847 bli-1(n361) mutant which produces abnormal cuticle blisters. *Cell Tissue Res.* **2003**, *312*, 229–235. [[CrossRef](#)]
116. Schultz, R.D.; Bennett, E.E.; Ellis, E.A.; Gumienny, T.L. Regulation of extracellular matrix organization by BMP signaling in *Caenorhabditis elegans*. *PLoS ONE* **2014**, *9*, e101929. [[CrossRef](#)]
117. Schultz, R.D.; Gumienny, T.L. Visualization of *Caenorhabditis elegans* cuticular structures using the lipophilic vital dye DiI. *J. Vis. Exp.* **2012**, *59*, e3362. [[CrossRef](#)]
118. Li, Y.; Paik, Y.K. A potential role for fatty acid biosynthesis genes during molting and cuticle formation in *Caenorhabditis elegans*. *BMB Rep.* **2011**, *44*, 285–290. [[CrossRef](#)]
119. Van de Walle, P.; Geens, E.; Baggerman, G.; Jose Naranjo-Galindo, F.; Askjaer, P.; Schoofs, L.; Temmerman, L. CEH-60/PBX regulates vitellogenesis and cuticle permeability through intestinal interaction with UNC-62/MEIS in *Caenorhabditis elegans*. *PLoS Biol.* **2019**, *17*, e3000499. [[CrossRef](#)]

120. Boshier, J.M.; Hahn, B.S.; Legouis, R.; Sookhareea, S.; Weimer, R.M.; Gansmuller, A.; Labouesse, M. The *Caenorhabditis elegans* vab-10 spectraplaklin isoforms protect the epidermis against internal and external forces. *J. Cell Biol.* **2003**, *161*, 757–768. [[CrossRef](#)]
121. Zhang, H.; Labouesse, M. The making of hemidesmosome structures in vivo. *Dev. Dyn.* **2010**, *239*, 1465–1476. [[CrossRef](#)]
122. Gotenstein, J.R.; Koo, C.C.; Ho, T.W.; Chisholm, A.D. Genetic Suppression of Basement Membrane Defects in *Caenorhabditis elegans* by Gain of Function in Extracellular Matrix and Cell-Matrix Attachment Genes. *Genetics* **2018**, *208*, 1499–1512. [[CrossRef](#)]
123. McMahan, L.; Muriel, J.M.; Roberts, B.; Quinn, M.; Johnstone, I.L. Two sets of interacting collagens form functionally distinct substructures within a *Caenorhabditis elegans* extracellular matrix. *Mol. Biol. Cell* **2003**, *14*, 1366–1378. [[CrossRef](#)]
124. Dodd, W.; Tang, L.; Lone, J.C.; Wimberly, K.; Wu, C.W.; Consalvo, C.; Choe, K.P. A Damage Sensor Associated with the Cuticle Coordinates Three Core Environmental Stress Responses in *Caenorhabditis elegans*. *Genetics* **2018**, *208*, 1467–1482. [[CrossRef](#)] [[PubMed](#)]
125. Zhang, Y.; Li, W.; Li, L.; Li, Y.; Fu, R.; Zhu, Y.; Zhang, H. Structural damage in the *C. elegans* epidermis causes release of STA-2 and induction of an innate immune response. *Immunity* **2015**, *42*, 309–320. [[CrossRef](#)] [[PubMed](#)]
126. Zhang, Y.; Qi, L.; Zhang, H. TGF β -like DAF-7 acts as a systemic signal for autophagy regulation in *C. elegans*. *J. Cell Biol.* **2019**, *218*, 3998–4006. [[CrossRef](#)]
127. Lassandro, F.; Sebastiano, M.; Zei, F.; Bazzicalupo, P. The role of dityrosine formation in the crosslinking of CUT-2, the product of a second cuticlin gene of *Caenorhabditis elegans*. *Mol. Biochem. Parasitol.* **1994**, *65*, 147–159. [[CrossRef](#)]
128. Muriel, J.M.; Brannan, M.; Taylor, K.; Johnstone, I.L.; Lithgow, G.J.; Tuckwell, D. M142.2 (cut-6), a novel *Caenorhabditis elegans* matrix gene important for dauer body shape. *Dev. Biol.* **2003**, *260*, 339–351. [[CrossRef](#)]
129. Sebastiano, M.; Lassandro, F.; Bazzicalupo, P. cut-1 a *Caenorhabditis elegans* gene coding for a dauer-specific noncollagenous component of the cuticle. *Dev. Biol.* **1991**, *146*, 519–530. [[CrossRef](#)]
130. Flatt, K.M.; Beshers, C.; Unal, C.; Cohen, J.D.; Sundaram, M.V.; Schroeder, N.E. Epidermal Remodeling in *Caenorhabditis elegans* Dauers Requires the Nidogen Domain Protein DEX-1. *Genetics* **2019**, *211*, 169–183. [[CrossRef](#)]
131. Meli, V.S.; Osuna, B.; Ruvkun, G.; Frand, A.R. MLT-10 defines a family of DUF644 and proline-rich repeat proteins involved in the molting cycle of *Caenorhabditis elegans*. *Mol. Biol. Cell* **2010**, *21*, 1648–1661. [[CrossRef](#)]
132. Brenner, S. The genetics of *Caenorhabditis elegans*. *Genetics* **1974**, *77*, 71–94. [[PubMed](#)]
133. Noble, L.M.; Miah, A.; Kaur, T.; Rockman, M.V. The Ancestral *Caenorhabditis elegans* Cuticle Suppresses rol-1. *G3* **2020**, *10*, 2385–2395. [[CrossRef](#)] [[PubMed](#)]
134. Fernando, T.; Flibotte, S.; Xiong, S.; Yin, J.; Yzeiraj, E.; Moerman, D.G.; Savage-Dunn, C. *C. elegans* ADAMTS ADT-2 regulates body size by modulating TGF β signaling and cuticle collagen organization. *Dev. Biol.* **2011**, *352*, 92–103. [[CrossRef](#)] [[PubMed](#)]
135. Maduzia, L.L.; Gumienny, T.L.; Zimmerman, C.M.; Wang, H.; Shetgiri, P.; Krishna, S.; Padgett, R.W. lon-1 regulates *Caenorhabditis elegans* body size downstream of the dbl-1 TGF beta signaling pathway. *Dev. Biol.* **2002**, *246*, 418–428. [[CrossRef](#)]
136. Morita, K.; Chow, K.L.; Ueno, N. Regulation of body length and male tail ray pattern formation of *Caenorhabditis elegans* by a member of TGF-beta family. *Development* **1999**, *126*, 1337–1347.
137. Nyström, J.; Shen, Z.Z.; Aili, M.; Flemming, A.J.; Leroi, A.; Tuck, S. Increased or decreased levels of *Caenorhabditis elegans* lon-3, a gene encoding a collagen, cause reciprocal changes in body length. *Genetics* **2002**, *161*, 83–97.
138. Suzuki, Y.; Morris, G.A.; Han, M.; Wood, W.B. A cuticle collagen encoded by the lon-3 gene may be a target of TGF-beta signaling in determining *Caenorhabditis elegans* body shape. *Genetics* **2002**, *162*, 1631–1639.
139. Clark, J.F.; Meade, M.; Ranepura, G.; Hall, D.H.; Savage-Dunn, C. *Caenorhabditis elegans* DBL-1/BMP Regulates Lipid Accumulation via Interaction with Insulin Signaling. *G3 (Bethesda)* **2018**, *8*, 343–351. [[CrossRef](#)]
140. Savage-Dunn, C.; Padgett, R.W. The TGF- β Family in *Caenorhabditis elegans*. *Cold Spring Harb. Perspect. Biol.* **2017**, *9*. [[CrossRef](#)]

141. Madaan, U.; Yzeiraj, E.; Meade, M.; Clark, J.F.; Rushlow, C.A.; Savage-Dunn, C. BMP Signaling Determines Body Size via Transcriptional Regulation of Collagen Genes in *Caenorhabditis elegans*. *Genetics* **2018**, *210*, 1355–1367. [[CrossRef](#)]
142. Madaan, U.; Faure, L.; Chowdhury, A.; Ahmed, S.; Ciccarelli, E.J.; Gumienny, T.L.; Savage-Dunn, C. Feedback regulation of BMP signaling by *Caenorhabditis elegans* cuticle collagens. *Mol. Biol. Cell* **2020**, *31*, 825–832. [[CrossRef](#)] [[PubMed](#)]
143. Meng, X.M.; Nikolic-Paterson, D.J.; Lan, H.Y. TGF- β : The master regulator of fibrosis. *Nat. Rev. Nephrol.* **2016**, *12*, 325–338. [[CrossRef](#)] [[PubMed](#)]
144. Wright, K.A.; Thomson, J.N. The buccal capsule of *Caenorhabditis elegans* (Nematoda: Rhabditoidea): An ultrastructural study. *Can. J. Zool.* **1981**, *59*, 1952–1961. [[CrossRef](#)]
145. Drace, K.; McLaughlin, S.; Darby, C. *Caenorhabditis elegans* BAH-1 is a DUF23 protein expressed in seam cells and required for microbial biofilm binding to the cuticle. *PLoS ONE* **2009**, *4*, e6741. [[CrossRef](#)] [[PubMed](#)]
146. Hodgkin, J.; Clark, L.C.; Gravato-Nobre, M.J. Worm-stars and half-worms: Novel dangers and novel defense. *Worm* **2014**, *3*, e27939. [[CrossRef](#)] [[PubMed](#)]
147. Sulston, J.E.; Albertson, D.G.; Thomson, J.N. The *Caenorhabditis elegans* male: Postembryonic development of nongonadal structures. *Dev. Biol.* **1980**, *78*, 542–576. [[CrossRef](#)]
148. Sulston, J.E.; Horvitz, H.R. Post-embryonic cell lineages of the nematode, *Caenorhabditis elegans*. *Dev. Biol.* **1977**, *56*, 110–156. [[CrossRef](#)]
149. Yu, R.Y.; Nguyen, C.Q.; Hall, D.H.; Chow, K.L. Expression of ram-5 in the structural cell is required for sensory ray morphogenesis in *Caenorhabditis elegans* male tail. *EMBO J.* **2000**, *19*, 3542–3555. [[CrossRef](#)]
150. Soete, G.; Betist, M.C.; Korswagen, H.C. Regulation of *Caenorhabditis elegans* body size and male tail development by the novel gene lon-8. *BMC Dev. Biol.* **2007**, *7*, 20. [[CrossRef](#)]
151. Baird, S.E.; Emmons, S.W. Properties of a class of genes required for ray morphogenesis in *Caenorhabditis elegans*. *Genetics* **1990**, *126*, 335–344.
152. Kuno, K.; Baba, C.; Asaka, A.; Matsushima, C.; Matsushima, K.; Hosono, R. The *Caenorhabditis elegans* ADAMTS family gene adt-1 is necessary for morphogenesis of the male copulatory organs. *J. Biol. Chem.* **2002**, *277*, 12228–12236. [[CrossRef](#)] [[PubMed](#)]
153. Ko, F.C.; Chow, K.L. A novel thioredoxin-like protein encoded by the *C. elegans* dpy-11 gene is required for body and sensory organ morphogenesis. *Development* **2002**, *129*, 1185–1194. [[PubMed](#)]
154. Ko, F.C.; Chow, K.L. A mutation at the start codon defines the differential requirement of dpy-11 in *Caenorhabditis elegans* body hypodermis and male tail. *Biochem. Biophys. Res. Commun.* **2003**, *309*, 201–208. [[CrossRef](#)]
155. Ko, F.C.; Chow, K.L. Mutations with sensory ray defect unmask cuticular glycoprotein antigens in *Caenorhabditis elegans* male tail. *Dev. Growth Differ.* **2000**, *42*, 69–77. [[CrossRef](#)] [[PubMed](#)]
156. Frand, A.R.; Russel, S.; Ruvkun, G. Functional genomic analysis of *C. elegans* molting. *PLoS Biol.* **2005**, *3*, e312. [[CrossRef](#)] [[PubMed](#)]
157. Hashmi, S.; Zhang, J.; Oksov, Y.; Lustigman, S. The *Caenorhabditis elegans* cathepsin Z-like cysteine protease, Ce-CPZ-1, has a multifunctional role during the worms' development. *J. Biol. Chem.* **2004**, *279*, 6035–6045. [[CrossRef](#)] [[PubMed](#)]
158. Stepek, G.; McCormack, G.; Birnie, A.J.; Page, A.P. The astacin metalloprotease moulting enzyme NAS-36 is required for normal cuticle ecdysis in free-living and parasitic nematodes. *Parasitology* **2011**, *138*, 237–248. [[CrossRef](#)] [[PubMed](#)]
159. Suzuki, M.; Sagoh, N.; Iwasaki, H.; Inoue, H.; Takahashi, K. Metalloproteases with EGF, CUB, and thrombospondin-1 domains function in molting of *Caenorhabditis elegans*. *Biol. Chem.* **2004**, *385*, 565–568. [[CrossRef](#)]
160. Joseph, B.B.; Wang, Y.; Edeen, P.; Lažetić, V.; Grant, B.D.; Fay, D.S. Control of clathrin-mediated endocytosis by NIMA family kinases. *PLoS Genet.* **2020**, *16*, e1008633. [[CrossRef](#)]
161. Yang, H.C.; Yu, H.; Liu, Y.C.; Chen, T.L.; Stern, A.; Lo, S.J.; Chiu, D.T. IDH-1 deficiency induces growth defects and metabolic alterations in GSPD-1-deficient *Caenorhabditis elegans*. *J. Mol. Med. (Berl.)* **2019**, *97*, 385–396. [[CrossRef](#)]
162. Miao, R.; Li, M.; Zhang, Q.; Yang, C.; Wang, X. An ECM-to-Nucleus Signaling Pathway Activates Lysosomes for *C. elegans* Larval Development. *Dev. Cell* **2020**, *52*, 21–37.e25. [[CrossRef](#)] [[PubMed](#)]

163. Soloviev, A.; Gallagher, J.; Marnef, A.; Kuwabara, P.E. *C. elegans* patched-3 is an essential gene implicated in osmoregulation and requiring an intact permease transporter domain. *Dev. Biol.* **2011**, *351*, 242–253. [[CrossRef](#)] [[PubMed](#)]
164. Perera, R.M.; Zoncu, R. The Lysosome as a Regulatory Hub. *Annu. Rev. Cell Dev. Biol.* **2016**, *32*, 223–253. [[CrossRef](#)] [[PubMed](#)]
165. Zha, J.; Ying, M.; Alexander-Floyd, J.; Gidalevitz, T. HSP-4/BiP expression in secretory cells is regulated by a developmental program and not by the unfolded protein response. *PLoS Biol.* **2019**, *17*, e3000196. [[CrossRef](#)]
166. Essmann, C.L.; Martinez-Martinez, D.; Pryor, R.; Leung, K.Y.; Krishnan, K.B.; Lui, P.P.; Cabreiro, F. Mechanical properties measured by atomic force microscopy define health biomarkers in ageing *C. elegans*. *Nat. Commun.* **2020**, *11*, 1043. [[CrossRef](#)]
167. Ewald, C.Y.; Landis, J.N.; Porter Abate, J.; Murphy, C.T.; Blackwell, T.K. Dauer-independent insulin/IGF-1-signalling implicates collagen remodelling in longevity. *Nature* **2015**, *519*, 97–101. [[CrossRef](#)]
168. Morikiri, Y.; Matsuta, E.; Inoue, H. The collagen-derived compound collagen tripeptide induces collagen expression and extends lifespan via a conserved p38 mitogen-activated protein kinase cascade. *Biochem. Biophys. Res. Commun.* **2018**, *505*, 1168–1173. [[CrossRef](#)]
169. Mesbahi, H.; Pho, K.B.; Tench, A.J.; Leon Guerrero, V.L.; MacNeil, L.T. Cuticle Collagen Expression Is Regulated in Response to Environmental Stimuli by the GATA Transcription Factor ELT-3 in *Caenorhabditis elegans*. *Genetics* **2020**, *215*, 483–495. [[CrossRef](#)]
170. Sellegounder, D.; Liu, Y.; Wibisono, P.; Chen, C.H.; Leap, D.; Sun, J. Neuronal GPCR NPR-8 regulates *C. elegans* defense against pathogen infection. *Sci. Adv.* **2019**, *5*, eaaw4717. [[CrossRef](#)]
171. Smit, R.B.; Schnabel, R.; Gaudet, J. The HLH-6 transcription factor regulates *C. elegans* pharyngeal gland development and function. *PLoS Genet.* **2008**, *4*, e1000222. [[CrossRef](#)]
172. Avery, L. The genetics of feeding in *Caenorhabditis elegans*. *Genetics* **1993**, *133*, 897–917. [[PubMed](#)]
173. Fang-Yen, C.; Avery, L.; Samuel, A.D. Two size-selective mechanisms specifically trap bacteria-sized food particles in *Caenorhabditis elegans*. *Proc. Natl. Acad. Sci. USA* **2009**, *106*, 20093–20096. [[CrossRef](#)] [[PubMed](#)]
174. Straud, S.; Lee, I.; Song, B.; Avery, L.; You, Y.J. The jaw of the worm: GTPase-activating protein EAT-17 regulates grinder formation in *Caenorhabditis elegans*. *Genetics* **2013**, *195*, 115–125. [[CrossRef](#)] [[PubMed](#)]
175. Sparacio, A.P.; Trojanowski, N.F.; Snetselaar, K.; Nelson, M.D.; Raizen, D.M. Teething during sleep: Ultrastructural analysis of pharyngeal muscle and cuticular grinder during the molt in *Caenorhabditis elegans*. *PLoS ONE* **2020**, *15*, e0233059. [[CrossRef](#)]
176. Stutz, K.; Kaech, A.; Aebi, M.; Künzler, M.; Hengartner, M.O. Disruption of the *C. elegans* Intestinal Brush Border by the Fungal Lectin CCL2 Phenocopies Dietary Lectin Toxicity in Mammals. *PLoS ONE* **2015**, *10*, e0129381. [[CrossRef](#)]
177. Knight, C.G.; Patel, M.N.; Azevedo, R.B.; Leroi, A.M. A novel mode of ecdysozoan growth in *Caenorhabditis elegans*. *Evol. Dev.* **2002**, *4*, 16–27. [[CrossRef](#)]
178. Park, J.O.; Pan, J.; Möhrlein, F.; Schupp, M.O.; Johnsen, R.; Baillie, D.L.; Hutter, H. Characterization of the astacin family of metalloproteases in *C. elegans*. *BMC Dev. Biol.* **2010**, *10*, 14. [[CrossRef](#)]
179. Bento, G.; Ogawa, A.; Sommer, R.J. Co-option of the hormone-signalling module dafachronic acid-DAF-12 in nematode evolution. *Nature* **2010**, *466*, 494–497. [[CrossRef](#)]
180. Bose, N.; Ogawa, A.; von Reuss, S.H.; Yim, J.J.; Ragsdale, E.J.; Sommer, R.J.; Schroeder, F.C. Complex small-molecule architectures regulate phenotypic plasticity in a nematode. *Angew. Chem. Int. Ed. Engl.* **2012**, *51*, 12438–12443. [[CrossRef](#)]
181. Sanghvi, G.V.; Baskaran, P.; Röseler, W.; Sieriebriennikov, B.; Rödelsperger, C.; Sommer, R.J. Life History Responses and Gene Expression Profiles of the Nematode *Pristionchus pacificus* Cultured on *Cryptococcus* Yeasts. *PLoS ONE* **2016**, *11*, e0164881. [[CrossRef](#)]
182. Werner, M.S.; Sieriebriennikov, B.; Loschko, T.; Namdeo, S.; Lenuzzi, M.; Dardiry, M.; Sommer, R.J. Environmental influence on *Pristionchus pacificus* mouth form through different culture methods. *Sci. Rep.* **2017**, *7*, 7207. [[CrossRef](#)] [[PubMed](#)]
183. Ragsdale, E.J.; Müller, M.R.; Rödelsperger, C.; Sommer, R.J. A developmental switch coupled to the evolution of plasticity acts through a sulfatase. *Cell* **2013**, *155*, 922–933. [[CrossRef](#)] [[PubMed](#)]
184. Sieriebriennikov, B.; Prabh, N.; Dardiry, M.; Witte, H.; Röseler, W.; Kieninger, M.R.; Sommer, R.J. A Developmental Switch Generating Phenotypic Plasticity Is Part of a Conserved Multi-gene Locus. *Cell Rep.* **2018**, *23*, 2835–2843.e4. [[CrossRef](#)] [[PubMed](#)]

185. Sieriebriennikov, B.; Sommer, R.J. Developmental Plasticity and Robustness of a Nematode Mouth-Form Polyphenism. *Front. Genet.* **2018**, *9*, 382. [[CrossRef](#)] [[PubMed](#)]
186. Waterston, R.; Ainscough, R.; Anderson, K.; Berks, M.; Blair, D.; Connell, M.; A Cooper, J.; Coulson, A.; Craxton, M.; Dear, S.; et al. The genome of the nematode *Caenorhabditis elegans*. *Cold Spring Harb. Symp. Quant. Biol.* **1993**, *58*, 367–376. [[CrossRef](#)] [[PubMed](#)]
187. Maduro, M.F. Gut development in *C. elegans*. *Semin. Cell Dev. Biol.* **2017**, *66*, 3–11. [[CrossRef](#)]
188. Geisler, F.; Coch, R.A.; Richardson, C.; Goldberg, M.; Bevilacqua, C.; Prevedel, R.; Leube, R.E. Intestinal intermediate filament polypeptides in *C. elegans*: Common and isotype-specific contributions to intestinal ultrastructure and function. *Sci. Rep.* **2020**, *10*, 3142. [[CrossRef](#)]
189. Schulenburg, H.; Félix, M.A. The Natural Biotic Environment of *Caenorhabditis elegans*. *Genetics* **2017**, *206*, 55–86. [[CrossRef](#)]
190. Maduzia, L.L.; Yu, E.; Zhang, Y. *Caenorhabditis elegans* galectins LEC-6 and LEC-10 interact with similar glycoconjugates in the intestine. *J. Biol. Chem.* **2011**, *286*, 4371–4381. [[CrossRef](#)]
191. Joshua, G.W. Functional analysis of leucine aminopeptidase in *Caenorhabditis elegans*. *Mol. Biochem. Parasitol.* **2001**, *113*, 223–232. [[CrossRef](#)]
192. Gravato-Nobre, M.J.; Vaz, F.; Filipe, S.; Chalmers, R.; Hodgkin, J. The Invertebrate Lysozyme Effector ILYS-3 Is Systemically Activated in Response to Danger Signals and Confers Antimicrobial Protection in *C. elegans*. *PLoS Pathog.* **2016**, *12*, e1005826. [[CrossRef](#)] [[PubMed](#)]
193. Julien-Gau, I.; Schmidt, M.; Kurz, C.L. f57f4.4p::gfp as a fluorescent reporter for analysis of the *C. elegans* response to bacterial infection. *Dev. Comp. Immunol.* **2014**, *42*, 132–137. [[CrossRef](#)] [[PubMed](#)]
194. Newman, A.P.; White, J.G.; Sternberg, P.W. Morphogenesis of the *C. elegans* hermaphrodite uterus. *Development* **1996**, *122*, 3617–3626. [[PubMed](#)]
195. Kubagawa, H.M.; Watts, J.L.; Corrigan, C.; Edmonds, J.W.; Sztul, E.; Browse, J.; Miller, M.A. Oocyte signals derived from polyunsaturated fatty acids control sperm recruitment in vivo. *Nat. Cell Biol.* **2006**, *8*, 1143–1148. [[CrossRef](#)] [[PubMed](#)]
196. McCaughey, J.; Stephens, D.J. ER-to-Golgi Transport: A Sizeable Problem. *Trends Cell Biol.* **2019**, *29*, 940–953. [[CrossRef](#)] [[PubMed](#)]
197. Roberts, B.; Clucas, C.; Johnstone, I.L. Loss of SEC-23 in *Caenorhabditis elegans* causes defects in oogenesis, morphogenesis, and extracellular matrix secretion. *Mol. Biol. Cell* **2003**, *14*, 4414–4426. [[CrossRef](#)]
198. McCaughey, J.; Stevenson, N.L.; Cross, S.; Stephens, D.J. ER-to-Golgi trafficking of procollagen in the absence of large carriers. *J. Cell Biol.* **2019**, *218*, 929–948. [[CrossRef](#)]
199. Zhang, Z.; Bai, M.; Barbosa, G.O.; Chen, A.; Wei, Y.; Luo, S.; Ma, D.K. Broadly conserved roles of TMEM131 family proteins in intracellular collagen assembly and secretory cargo trafficking. *Sci. Adv.* **2020**, *6*, eaay7667. [[CrossRef](#)]
200. Birchenough, G.M.; Johansson, M.E.; Gustafsson, J.K.; Bergström, J.H.; Hansson, G.C. New developments in goblet cell mucus secretion and function. *Mucosal Immunol.* **2015**, *8*, 712–719. [[CrossRef](#)]
201. Cohen, J.D.; Bermudez, J.G.; Good, M.C.; Sundaram, M.V. A *C. elegans* Zona Pellucida domain protein functions via its ZPc domain. *bioRxiv* **2020**. [[CrossRef](#)]
202. Hyenne, V.; Apaydin, A.; Rodriguez, D.; Spiegelhalter, C.; Hoff-Yoessle, S.; Diem, M.; Labouesse, M. RAL-1 controls multivesicular body biogenesis and exosome secretion. *J. Cell Biol.* **2015**, *211*, 27–37. [[CrossRef](#)] [[PubMed](#)]
203. Kolotuev, I.; Schwab, Y.; Labouesse, M. A precise and rapid mapping protocol for correlative light and electron microscopy of small invertebrate organisms. *Biol. Cell* **2009**, *102*, 121–132. [[CrossRef](#)] [[PubMed](#)]
204. Liégeois, S.; Benedetto, A.; Garnier, J.M.; Schwab, Y.; Labouesse, M. The V0-ATPase mediates apical secretion of exosomes containing Hedgehog-related proteins in *Caenorhabditis elegans*. *J. Cell Biol.* **2006**, *173*, 949–961. [[CrossRef](#)] [[PubMed](#)]
205. Barczyk, M.; Carracedo, S.; Gullberg, D. Integrins. *Cell Tissue Res.* **2010**, *339*, 269–280. [[CrossRef](#)] [[PubMed](#)]
206. Cao, X.; Surma, M.A.; Simons, K. Polarized sorting and trafficking in epithelial cells. *Cell Res.* **2012**, *22*, 793–805. [[CrossRef](#)] [[PubMed](#)]
207. Dervedde, J.; Weise, C.; Muller, E.C.; Hagiwara, A.; Bachmann, S.; Suzuki, M.; Scherer, H. Cupulin is a zona pellucida-like domain protein and major component of the cupula from the inner ear. *PLoS ONE* **2014**, *9*, e111917. [[CrossRef](#)]

208. Devuyst, O.; Olinger, E.; Rampoldi, L. Uromodulin: From physiology to rare and complex kidney disorders. *Nat. Rev. Nephrol.* **2017**, *13*, 525–544. [[CrossRef](#)]
209. Gupta, S.K. The Human Egg's Zona Pellucida. *Curr. Top. Dev. Biol.* **2018**, *130*, 379–411. [[CrossRef](#)]
210. Liaskos, C.; Rigopoulou, E.I.; Orfanidou, T.; Bogdanos, D.P.; Papandreou, C.N. CUZD1 and anti-CUZD1 antibodies as markers of cancer and inflammatory bowel diseases. *Clin. Dev. Immunol.* **2013**, *2013*, 968041. [[CrossRef](#)]
211. McAllister, K.A.; Grogg, K.M.; Johnson, D.W.; Gallione, C.J.; Baldwin, M.A.; Jackson, C.E.; Helmbold, E.A.; Markel, D.S.; McKinnon, W.C.; Murrell, J. Endoglin, a TGF-beta binding protein of endothelial cells, is the gene for hereditary haemorrhagic telangiectasia type 1. *Nat. Genet.* **1994**, *8*, 345–351. [[CrossRef](#)]
212. Roggenbuck, D.; Hausdorf, G.; Martinez-Gamboa, L.; Reinhold, D.; Büttner, T.; Jungblut, P.R.; Porstmann, T.; Laass, M.W.; Henker, J.; Büning, C.; et al. Identification of GP2, the major zymogen granule membrane glycoprotein, as the autoantigen of pancreatic antibodies in Crohn's disease. *Gut* **2009**, *12*, 1620–1628. [[CrossRef](#)] [[PubMed](#)]
213. Judge, D.P.; Dietz, H.C. Marfan's syndrome. *Lancet* **2005**, *366*, 1965–1976. [[CrossRef](#)]
214. Kinsella, M.G.; Bressler, S.L.; Wight, T.N. The regulated synthesis of versican, decorin, and biglycan: Extracellular matrix proteoglycans that influence cellular phenotype. *Crit. Rev. Eukaryot. Gene Expr.* **2004**, *14*, 203–234. [[CrossRef](#)] [[PubMed](#)]
215. Flower, D.R. The lipocalin protein family: Structure and function. *Biochem. J.* **1996**, *318 Pt 1*, 1–14. [[CrossRef](#)]

Publisher's Note: MDPI stays neutral with regard to jurisdictional claims in published maps and institutional affiliations.



© 2020 by the authors. Licensee MDPI, Basel, Switzerland. This article is an open access article distributed under the terms and conditions of the Creative Commons Attribution (CC BY) license (<http://creativecommons.org/licenses/by/4.0/>).